UNCLASSIFIED

Security Classification

DOCUMENT CONTROL DATA - R & D

(Security classification of title, body of abstract and indexing annotation must be entered when the overall report is classified)

1. ORIGINATING ACTIVITY *(Corporate author)*

The University of Michigan Radiation Laboratory
2216 Space Research Bldg., North Campus
Ann Arbor, Michigan 48105

2a. REPORT SECURITY CLASSIFICATION

UNCLASSIFIED

2b. GROUP

3. REPORT TITLE

THEORETICAL AND EXPERIMENTAL STUDY OF ARRAYS OF AXIAL SLOTS ON A CIRCULAR CYLINDER

4. DESCRIPTIVE NOTES *(Type of report and inclusive dates)*

Final, Scientific For Period 1 September 1973 through 30 June 1974

5. AUTHOR(S) *(First name, middle initial, last name)*

Dipak L. Sengupta
Joseph E. Ferris

6. REPORT DATE	7a. TOTAL NO. OF PAGES	7b. NO. OF REFS
August 1974	43	4

8a. CONTRACT OR GRANT NO.	9a. ORIGINATOR'S REPORT NUMBER(S)
F19628-74-C-0020	
b. PROJECT NO. 5635-06-01	012131-1-F
c. 61102F	9b. OTHER REPORT NO(S) *(Any other numbers that may be assigned this report)*
d. 681305	AFCRL-TR-74-0420

10. DISTRIBUTION STATEMENT

Approved for public release; distribution unlimited.

11. SUPPLEMENTARY NOTES	12. SPONSORING MILITARY ACTIVITY
Tech. Other	Air Force Cambridge Research Laboratories Hanscom AFB, Massachusetts 01731 Contract Monitor: Otho E. Kerr/LZR

13. ABSTRACT

The radiation patterns produced by arrays of axial slots on a conducting circular cylinder of infinite length are studied theoretically and experimentally. The required phase of excitation of elements to produce a beam in a certain direction are obtained by approximating the array by a section of a circular array of isotropic sources. For the given radius of the cylinder and the frequency band of interest, the approximation is found to yield satisfactory results. Radiation patterns produced by arrays of 2, 3 and 4 axial slots are numerically computed and discussed. Theoretical results are also compared with measured results and the agreement between the two has been found satisfactory.

DD FORM 1 NOV 65 1473

UNCLASSIFIED

Security Classification

14. KEY WORDS	LINK A		LINK B		LINK C	
	ROLE	WT	ROLE	WT	ROLE	WT
Single Beam Antennas						
Slot Arrays on Circular Cylinder						
Radiation Patterns of Slot Arrays						
VSWR of Slot Arrays						

TABLE OF CONTENTS

I. INTRODUCTION

1.1 Preliminary Remarks

The objective of the research reported herein is to determine the best arrangement of elements for an antenna to produce a single beam pattern for applications on electrically small aircraft or missiles. The antenna is to operate in the low VHF range (30 MHz - 200 MHz; λ = 10 m - 1.5 m). The electrically small vehicle is approximated by a perfectly conducting circular cylinder of diamter $\sim$ 2 meters and length $\sim$13 meters. For obtaining patterns in a plane normal to the axis of the cylinder produced by elementary slot radiators placed on its surface, the cylinder is assumed to be of infinite length. This assumption simplifies the theoretical analysis considerably.

1.2 General Considerations

Let us represent the fuselage of the aircraft by a conducting infinite cylinder of radius a . The coordinate system used and the orientation of the system are shown in Figure 1 where the axis of the cylinder is oriented along the z-axis. We shall refer to the x-y plane as the vertical or elevation plane, the y-z plane as the horizontal plane and the x-z plane as the longitudinal plane.

The desired beam produced by the antenna should be normal to the z-axis and be directed as shown in Figure 1. The antenna should also have some directivity in the y-z plane. Ideally, there should not be any radiation beyond the range

$$\phi_o - \frac{\Delta\phi_o}{2} \leq \phi \leq \phi_o + \frac{\Delta\phi_o}{2} ,$$

where $\Delta\phi_o$ is the beamwidth between nulls in the x-y plane pattern.

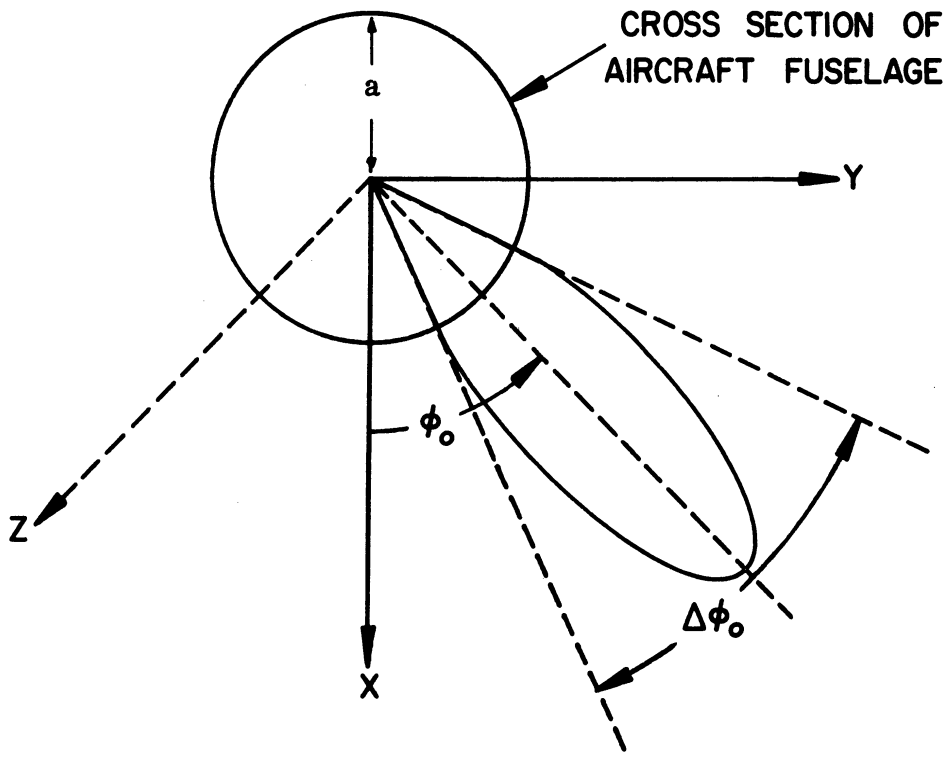

Figure 1: Idealized pattern and the coordinate system used.

We assume here that the sidelobe levels, if any, should be about 15 to 20dB down from the main beam.

The antenna system should have a bandwidth of 5 MHz with a VSWR equal to 3.0:1. This implies that at 30 MHz the required bandwidth would be about $\pm$ 8 p.c. and about $\pm$ 1.25 p.c. at 200 MHz.

The bandwidth requirements at the lower frequency end appears to be quite severe. From this consideration alone it may be advisable to use antennas such as the log-periodic, the yagi or zig-zag antennas. If circular polarization is acceptable one may also consider the use of flat spiral, conical spiral or

helical antennas. However, all these antennas would require an excessive amount of protrusion from the cylinder or require a large amount of cylindrical surface area at the lower frequency end. Because of this we have ruled out the use of such antennas for the present study.

To obtain the desired patterns we use the technique of arraying a number of elementary radiators around the circular cylinder. Axial slot radiators are considered for the reason that they need minimum amount of protrusion from the cylinder surface.

1.3 Outline of the Report

In Chapter II we derive the expressions for the desired far field patterns produced by arrays of axial slots on a conducting circular cylinder of infinite length. The required phase of excitation of elements to produce a beam in a certain direction are obtained by assuming that the array consists of a section of a circular array of isotropic sources. For the given radius of the cylinder and the frequency band of interest, the approximation is found to yield satisfactory results. Radiation patterns produced by arrays of 2, 3 and 4 slots on the circular cylinder are numerically computed and discussed.

Chapter III discusses the experimental results. The agreement between the theoretical and experimental results are found to be satisfactory.

II. THEORETICAL AND NUMERICAL ANSLYSIS

In this chapter we develop theoretical expressions for the radiation field produced by a number of axial slots located on the surface of a conducting circular cylinder of infinite length. The far field patterns produced by such elementary radiators are discussed thoroughly in the literature [1 - 3]. Here we write them in a manner suitable for our purpose and use them to obtain the array pattern expressions. The radiation patterns produced by arrays of monopoles or stub radiators located on a circular cylinder have been discussed in our first quarterly report [4] and will not be repeated here.

2.1 Theoretical Pattern Expressions

Consider a narrow axial slot of length L located on the surface of the cylinder at $\phi = \phi_\ell$ and $z = 0$ as shown in Figure 2. Let the excitation of the slot be represented by:

$$\vec{E}_s = \frac{V_\ell e^{i\psi_\ell}}{2a\,\Delta\phi} \cos\frac{\pi a}{L}\,\hat{e}_\phi \,, \tag{1}$$

where,

V_ℓ ψ_ℓ are the amplitude and phase of the excitation,

$2\Delta\phi$ is the width of the slot,

$e^{-i\omega t}$ is the assumed time dependence,

$\hat{e}_\phi$ is the unit vector in the ϕ-direction.

It can be shown [2] that the far electric field produced by such a slot of length $L = \lambda/2$ has only a ϕ-component and is given by:

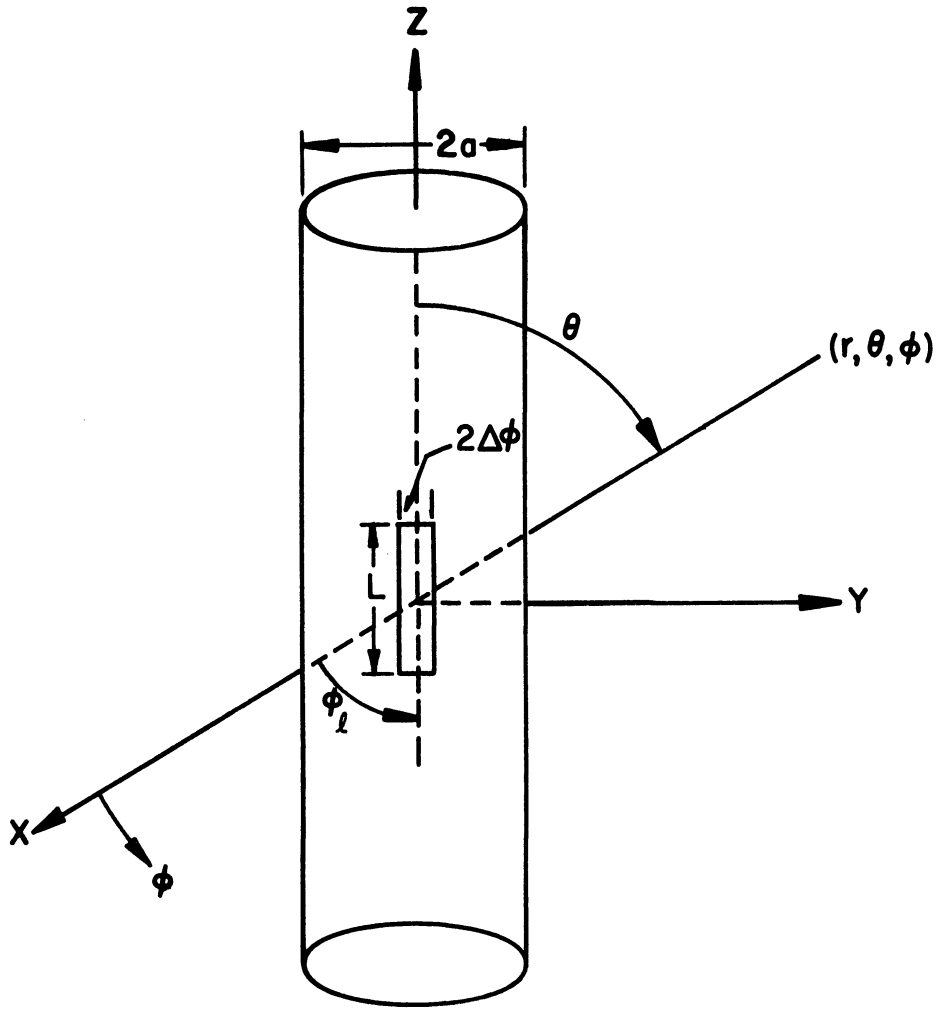

Figure 2: Axial slot on a circular cylinder and the coordinate system used.

$$E_{\phi} = \frac{e^{ikr}}{r} \frac{V_{\ell} e^{i\psi_{\ell}}}{\pi^2 (ka)} \frac{\cos\left(\frac{\pi}{2}\cos\theta\right)}{\sin\theta} \times$$

$$\times \sum_{n=0}^{\infty} \frac{\epsilon_n (-i)^n \cos n(\phi - \phi_{\ell})}{\sin\theta \, H_n^{(1)'}(ka \sin\theta)} \frac{\sin n\Delta\phi}{n\Delta\phi}, \qquad (2)$$

where,

$k = \frac{\omega}{c}$ is the propagation constant in free space,

r, θ, ϕ are the usual sphereical coordinates,

$H_n^{(1)}$ represents Hankel function of the first kind and order n,

$'$ indicates differentiation with respect to the argument,

$\epsilon_n = 1$ for $n = 0$

$= 2$ for $n \neq 0$.

For a narrow slot, $\Delta \phi \simeq 0$, so that we can assume $\frac{\sin n \Delta \phi}{n \Delta \phi} \simeq 1$ in Equation (2). Thus the far field in the x-y plane ($\theta = \pi/2$) may be represented by:

$$E_\phi = \frac{e^{ikr}}{r} P_\ell(\phi) ,$$

where,

$$P_\ell(\phi) = \frac{1}{\pi^2 (ka)} V_\ell e^{i\psi_\ell} \sum_{n=0}^{\infty} \frac{\epsilon_n (-1)^n \cos n (\phi - \phi_\ell)}{H_n^{(1)'}(ka)} \quad . \tag{4}$$

$\left| P_\ell(\phi) \right|$ is the x-y plane pattern produced by a single axial slot located at $\phi = \phi_\ell$. The pattern produced by an array of such slots located on the cylinder may be obtained by summing Equation (4) over the index ℓ and may be written formally as:

$$P(\phi) = \sum_\ell P_\ell(\phi) \quad . \tag{5}$$

Equation (5) assumes that there is no mutual coupling between the slots which would be a valid approximation as long as the slots are not too close to each other. In our analysis we neglect the mutual coupling between the slots.

2.2 Excitation of the Array

It has been assumed in the previous section that the array is obtained by locating a number of axial slots on the cylinder at $z = 0$ plane and at $\phi = \phi_\ell$, the excitation of ℓ-th slot being $V_\ell e^{i\psi_\ell}$. Within the range of frequencies of interest and for the given size of the cylinder, it appears that the physical extent of the array should be confined approximately to one quarter of the cylinder circumference in order to obtain a desirable pattern. From this consideration it seems that the maximum number of slots that can be used for the array may be 4 or 5. For larger number of slots the mutual coupling effects would become appreciable and the analysis of the array pattern will be very complicated.

The array pattern expressions given by Equations (5) and (4) are in the form of double series, one of them being infinite. It is quite difficult, if not impossible, to obtain the array excitation coefficients V_ℓ, ψ_ℓ for a given beam direction from these series expressions.

We use the concepts of the section of a circular array of isotropic sources to obtain the excitation coefficients in the present case. Consider a section of a circular array of isotropic sources in the x-y plane, as shown in Figure 3. It can be shown that the far field pattern in the x-y plane is given by:

$$P(\phi) = \sum_\ell V_\ell e^{i\psi_\ell} \cdot e^{-ika \cos(\phi-\phi_\ell)}$$

$$= \sum_\ell V_\ell e^{-i\left[ka \cos(\phi-\phi_\ell) - \psi_\ell\right]} \qquad (6)$$

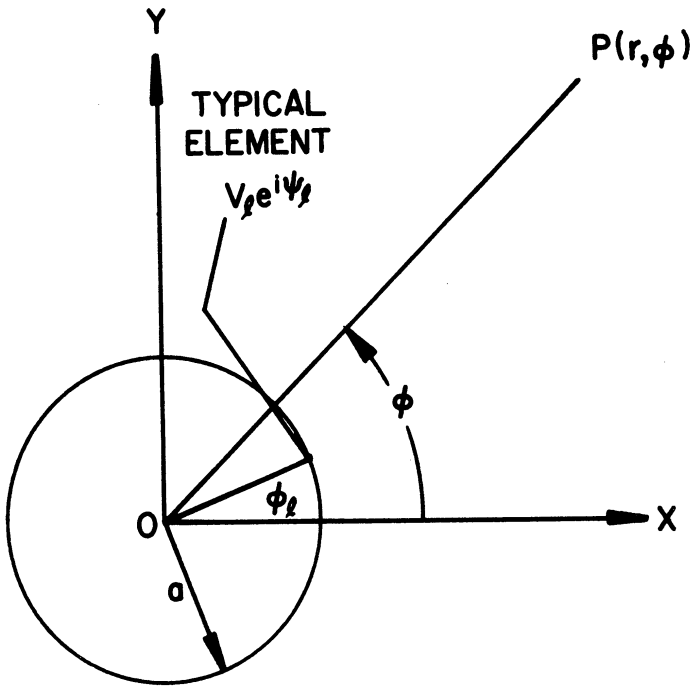

Figure 3: A circular section array with typical elements at $\phi = \phi_\ell$.

Let the desired direction of the beam maximum be $\phi = \phi_o$. Equation (6) indicates that the phase of the excitation ψ_ℓ must then satisfy the following:

$$ka \cos (\phi_o - \phi_\ell) = \psi_\ell \quad . \tag{7}$$

We shall design excitation coefficient ψ_ℓ for the slot array on the circular cylinder on the basis of Equation (7).

For example, let us design a 3-slot array which is required to produce maximum field in the direction $\phi_o = \pi/4$. For convenience we assume that the three slots are located at $\phi_1 = 0^o$, $\phi_2 = \pi/4$ and $\phi_3 = \pi/2$. The phase of excitation of the slots are then given by $\psi_1 = \frac{ka}{\sqrt{2}}$, $\psi_2 = ka$ and $\psi_3 = ka/\sqrt{2}$, respectively. If the slots are excited with uniform amplitude, $V_1 = V_2 = V_3 = 1$. It may be found necessary to use non-uniform amplitude of excitation to modify the pattern in directions away from the main beam.

2.3 Discussion of the Element Pattern Expression

The pattern produced by an individual slot element located on the cylinder is given by Equation (4) which is an infinite series. The convergence of the series depends on the parameter ka. Within the range of frequencies of interest the maximum value of ka is $\frac{4}{3}\pi$. It has been found that for proper convergence with ka = $\frac{4}{3}\pi$, it is necessary to consider at least ten terms in the series. Therefore in all of our pattern calculations we have used the first ten terms of Equation (4).

2.4 Numerical Results for Single Slot Radiation Patterns

In this section we discuss the far field patterns produced by an axial slot located on the surface of the conducting cylinder at $\phi_1 = 0^o$. The patterns have been obtained by numerical computation of Equation (4) for three selected values of ka. Figures 4(a)-(c) show the x-y plane patterns for three values of ka which correspond to the normalized radius ka of a cylinder of diameter 2m at 30 MHz, 60 MHz and 200 MHz respectively. It should be noted from Figure 4 that towards the lower end of the frequency band, the pattern is approximately isotropic over most of the range of ϕ. More importantly, it has been found from our numerical results, the phase of the radiation stays almost constant for small values of ka, and over an appreciable range of ϕ on either side of $\phi = 0^o$. This appears to justify the assumption of using isotropic sources for the calculation of the excitation coefficients for an array of such slots, as discussed in section 2.2.

2.5 Patterns of an Array of Two Slots

Figure 5 shows the pattern produced by a pair of axial slots located at $\phi_1 = 0^o$ and $\phi_2 = \pi/4$. The two slots are excited equally, i.e., $V_1 = V_2 = 1$ and $\psi_1 = \psi_2 = 0^o$. Observe that the beam maximum occurs at $\phi = \pi/4$ which is in agreement with Equation (7). Observe, also that the pattern maximum in the

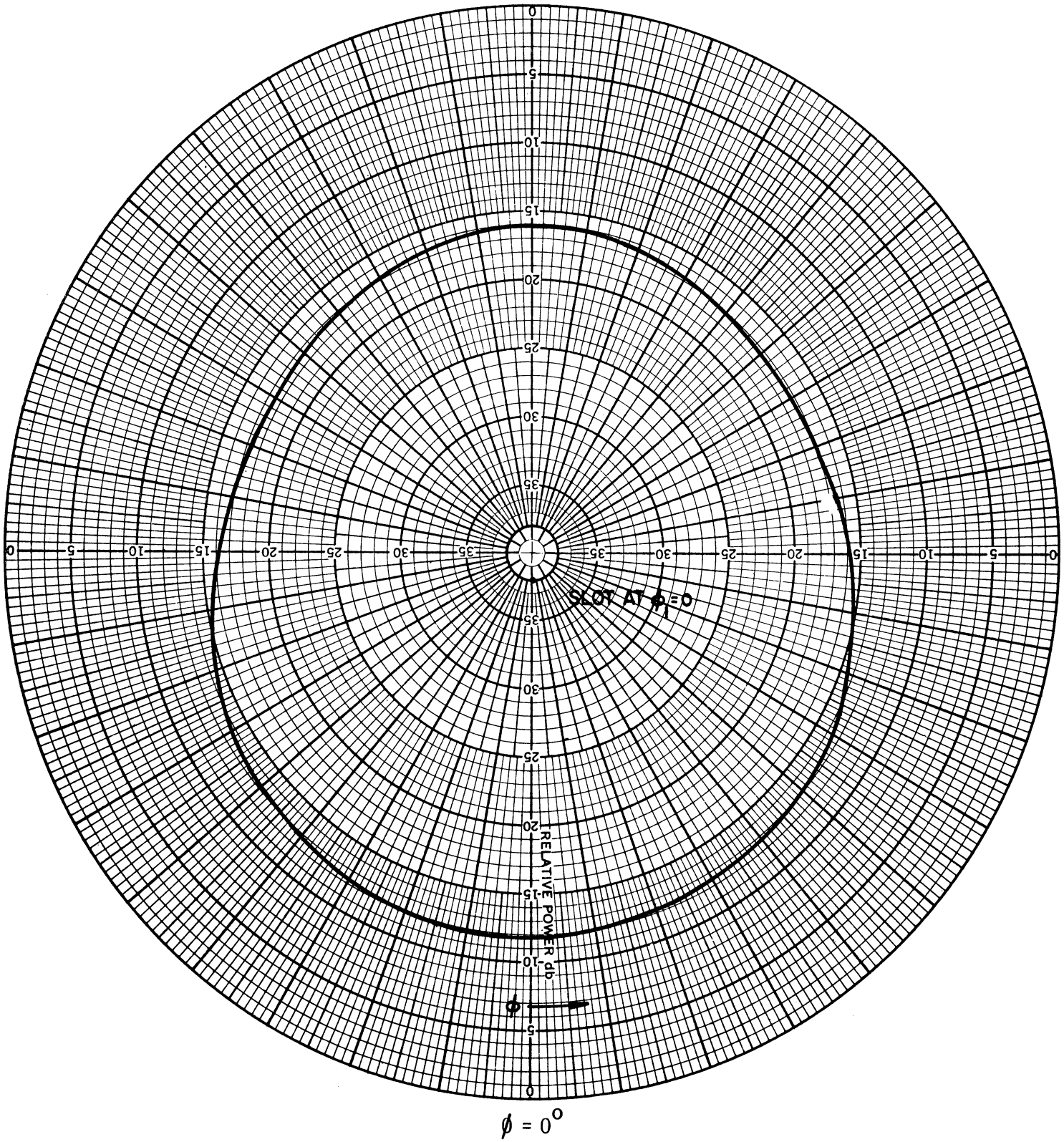

Figure 4(a): Theoretical pattern of an axial slot on the surface of a conducting cylinder, ka = 0.2π.

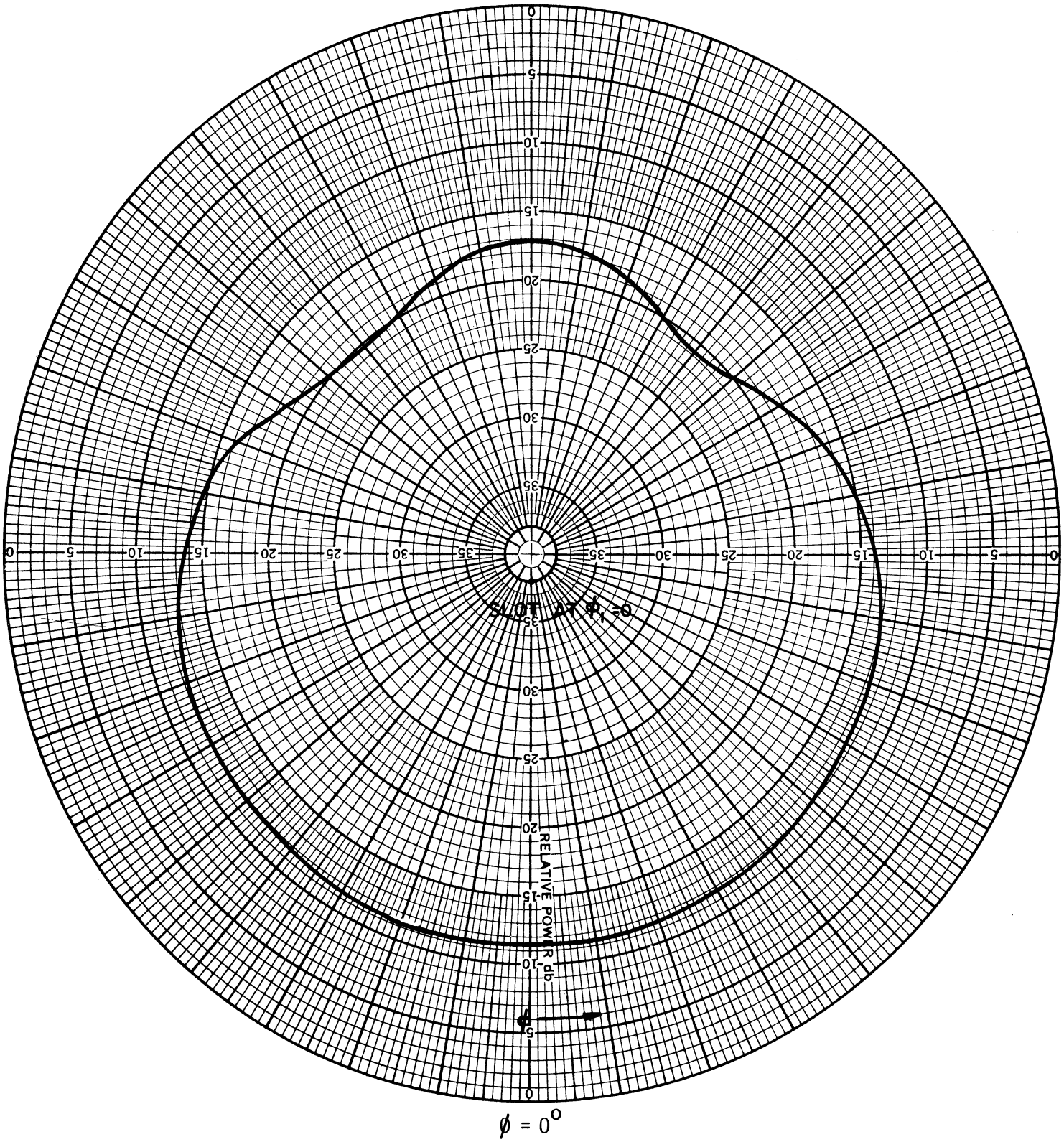

Figure 4(b): Theoretical pattern of an axial slot on the surface of a conducting cylinder, ka = 0.4π.

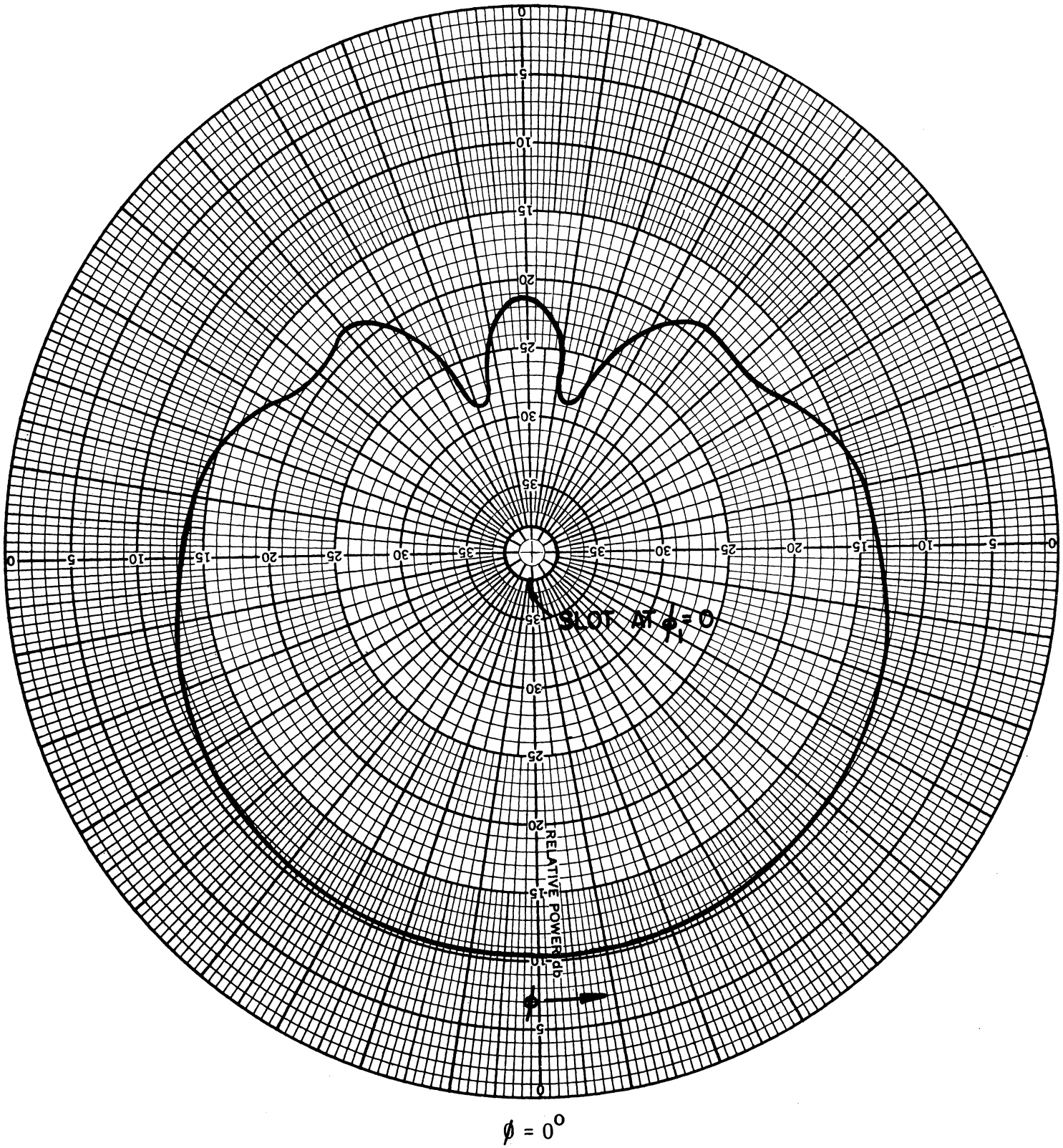

Figure 4(c): Theoretical pattern of an axial slot on the surface of a conducting cylinder, ka = $4/3\pi$.

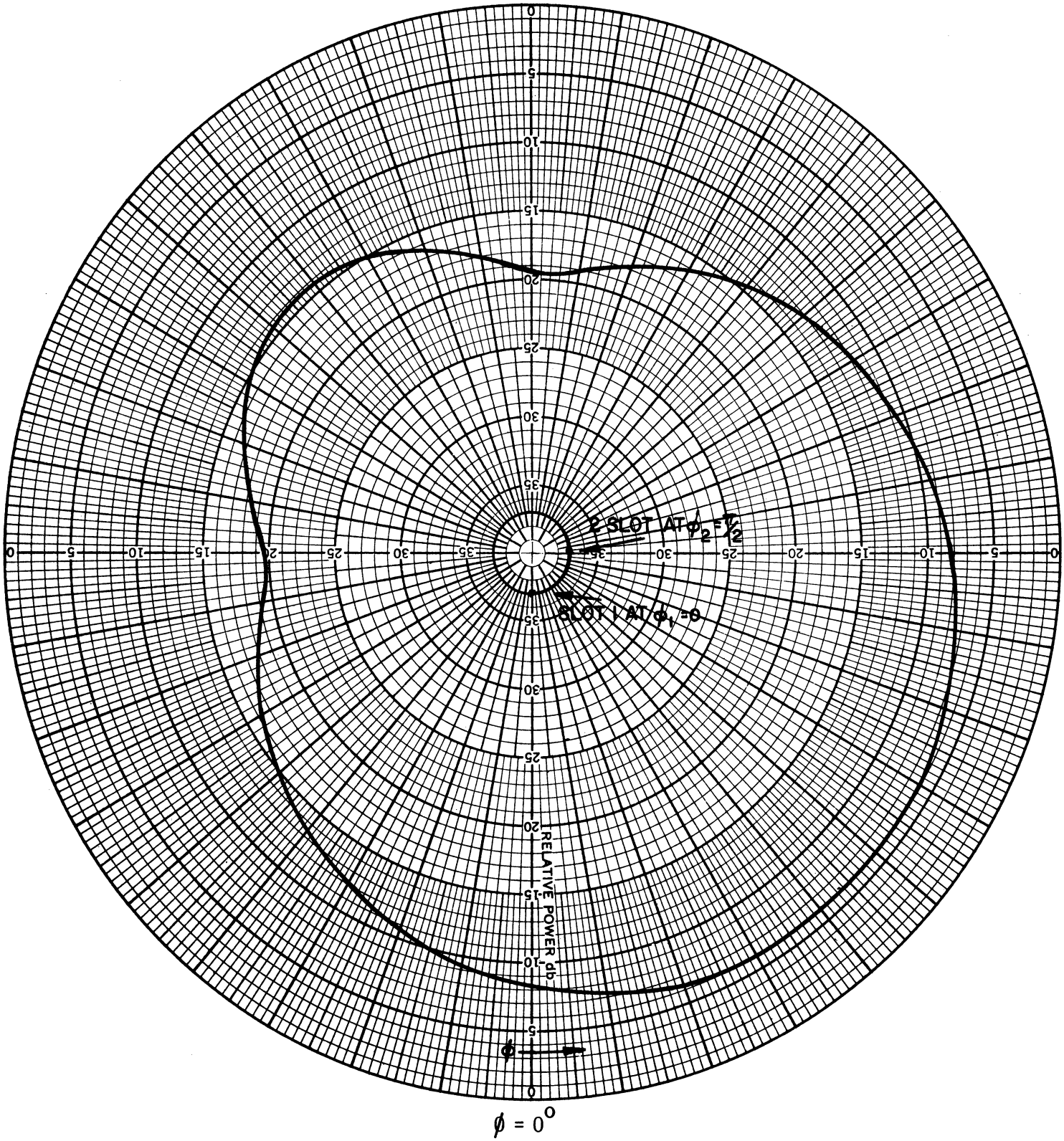

Figure 5: Theoretical pattern of a pair of equally excited axial slots located on the surface of a conducting cylinder, $ka = 0.4\pi$, $V_1 = V_2 = 1.0$, $\psi_1 = \psi_2 = 0^o$.

direction $\phi = \pi/4$ is about 15dB larger than that in the direction $\phi = 3\pi/2$. It appears from the results that by using third slot located at $\phi_3 = 3\pi/2$, the beam direction may be changed from $\phi = \pi/4$ to $\phi = -\pi/4$ by exciting slots 1 and 3 only.

2.6 Patterns of an Array of Three Slots

Figure 6 (a) - (c) show the patterns produced by an array of three axial slots located at $\phi_1 = 0^o$, $\phi_2 = \pi/4$ and $\phi_3 = \pi/2$ with uniform amplitude excitation, i.e., $V_1 = V_2 = V_3 = 1.0$. The phase of the excitation is chosen such that $\psi_1 = \psi_3 = ka/2$, $\psi_2 = ka$ obtained from Equation (7) for a beam maximum in the direction $\phi_o = \pi/4$. Figure 6 indicates that appreciable amount of directivity may be obtained in the upper half of the frequency band of interest.

Figure 7 (a)-(b) show the patterns produced by the same 3-slot array, but with non-uniform amplitude of excitation such that $V_1 = V_3 = 0.5$ and $V_2 = 1.0$. Comparing Figures 7 (a) and 6 (a), it is found that the patterns are quite similar. The pattern shown in Figure 7 (b) is for $ka = 0.707\pi$ and is found to be clean in the shadow side of the antenna. This may be found interesting for some applications.

2.7 Patterns of 4-Slot Array

The results discussed in the previous sections indicate that it is possible to obtain appreciable directivity in the upper end of the frequency band with a 3-slot antenna configuration. In general, it has been found that for such an array with $ka \simeq 0.8\pi$ the pattern has a principal maximum in the direction $\phi = 45^o$. In directions $\pm 90^o$ away from the main beam, the field is about 13dB down from the maximum (Figure 6 (b)). To reduce the field in the direction 90^o away from the main beam, we have used a fourth slot with proper exciation.

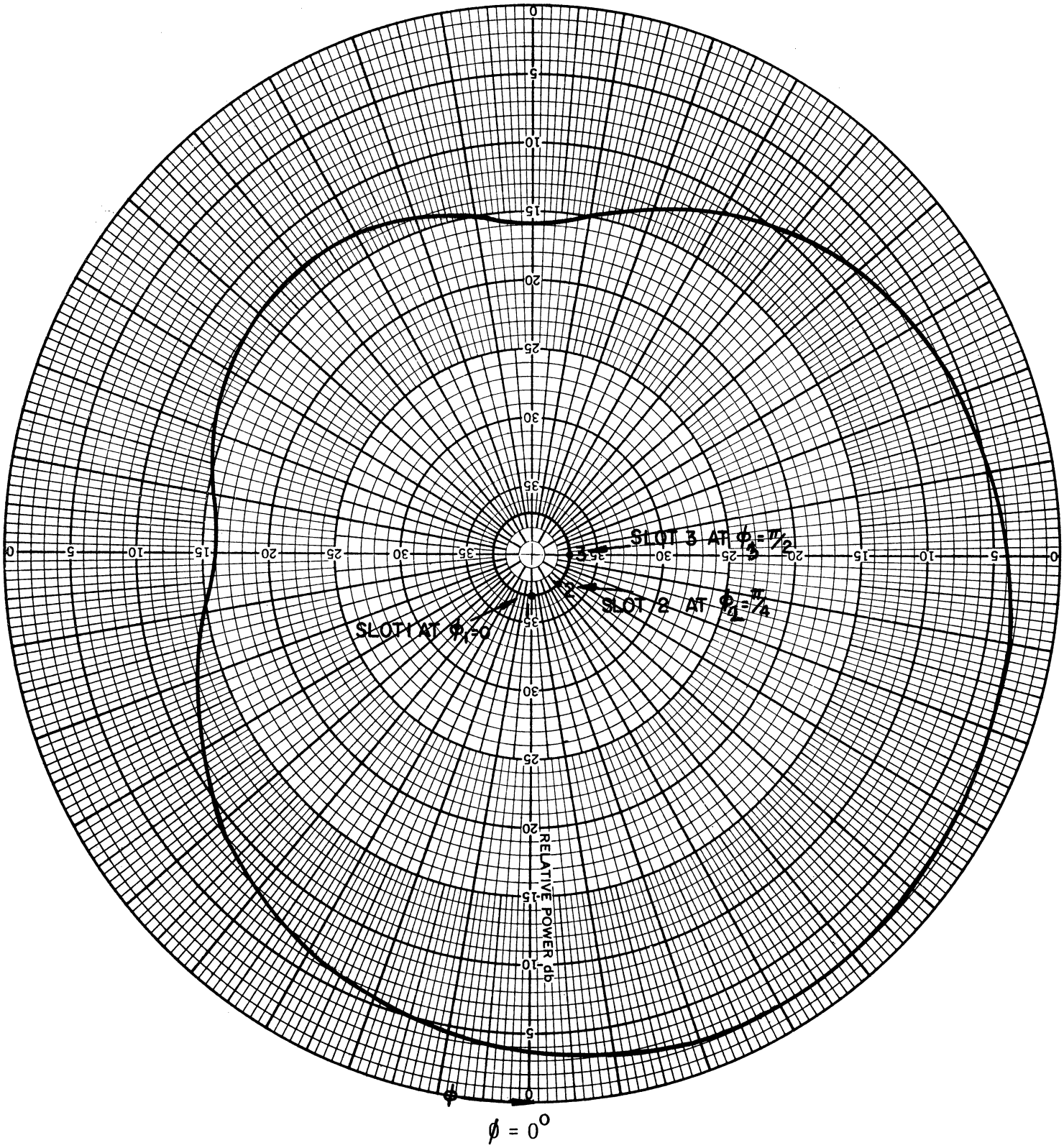

Figure 6(a): Theoretical pattern of three axial slots located on the surface of a conducting cylinder, $ka = 0.4\pi$, $V_1 = V_2 = V_3 = 1.0$, $\psi_2 = ka$, $\psi_1 = \psi_3 = ka/\sqrt{2}$.

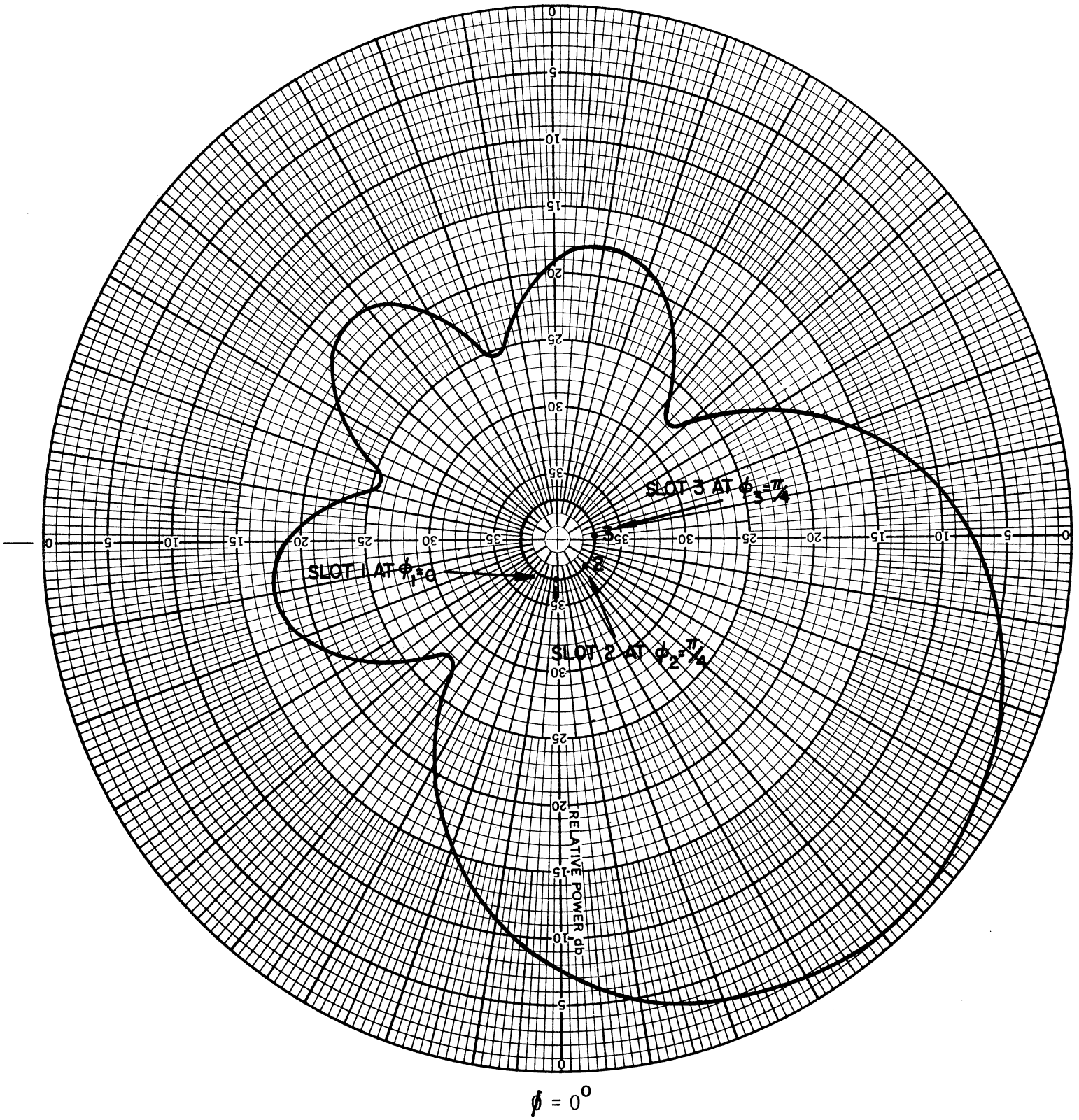

Figure 6(b): Theoretical pattern of three axial slots located on the surface of a conducting cylinder, ka = 0.8π, $V_1 = V_2 = V_3 = 1.0$, $\psi_2 = ka$, $\psi_1 = \psi_3 = ka/2$.

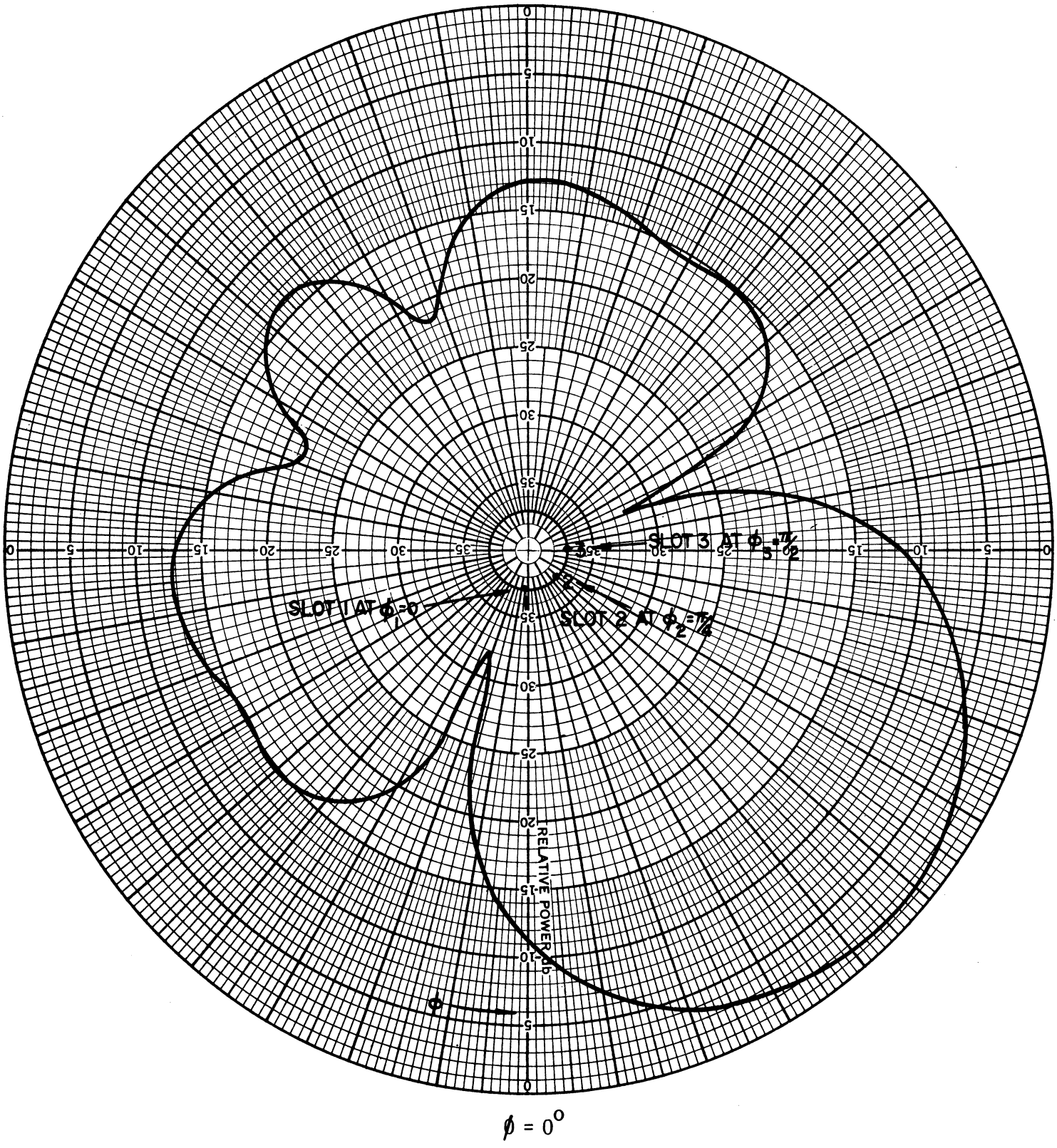

Figure 6(c): Theoretical pattern of three axial slots located on the surface of a conducting cylinder, ka = 1.0π, $V_1 = V_2 = V_3 = 1.0$, ψ_2 = ka, $\psi_1 = \psi_3$ = ka/$\sqrt{2}$.

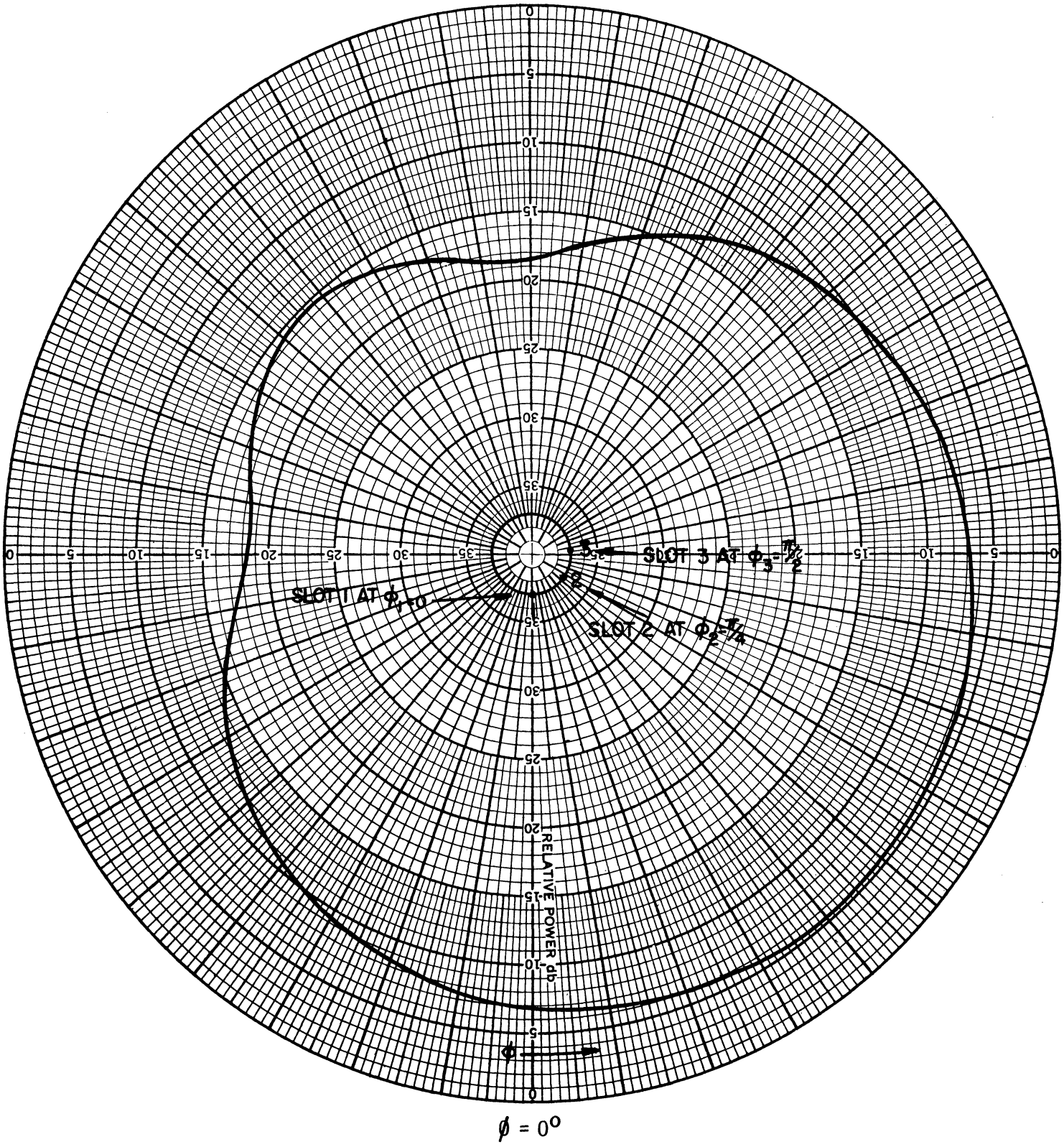

Figure 7(a): Theoretical pattern of three axial slots located on the surface of a conducting cylinder, ka = 0.4π, $V_1 = V_3 = 0.5$, $V_2 = 1.0$, $\psi_2 = ka$, $\psi_1 \doteq \psi_3 = ka/\sqrt{2}$.

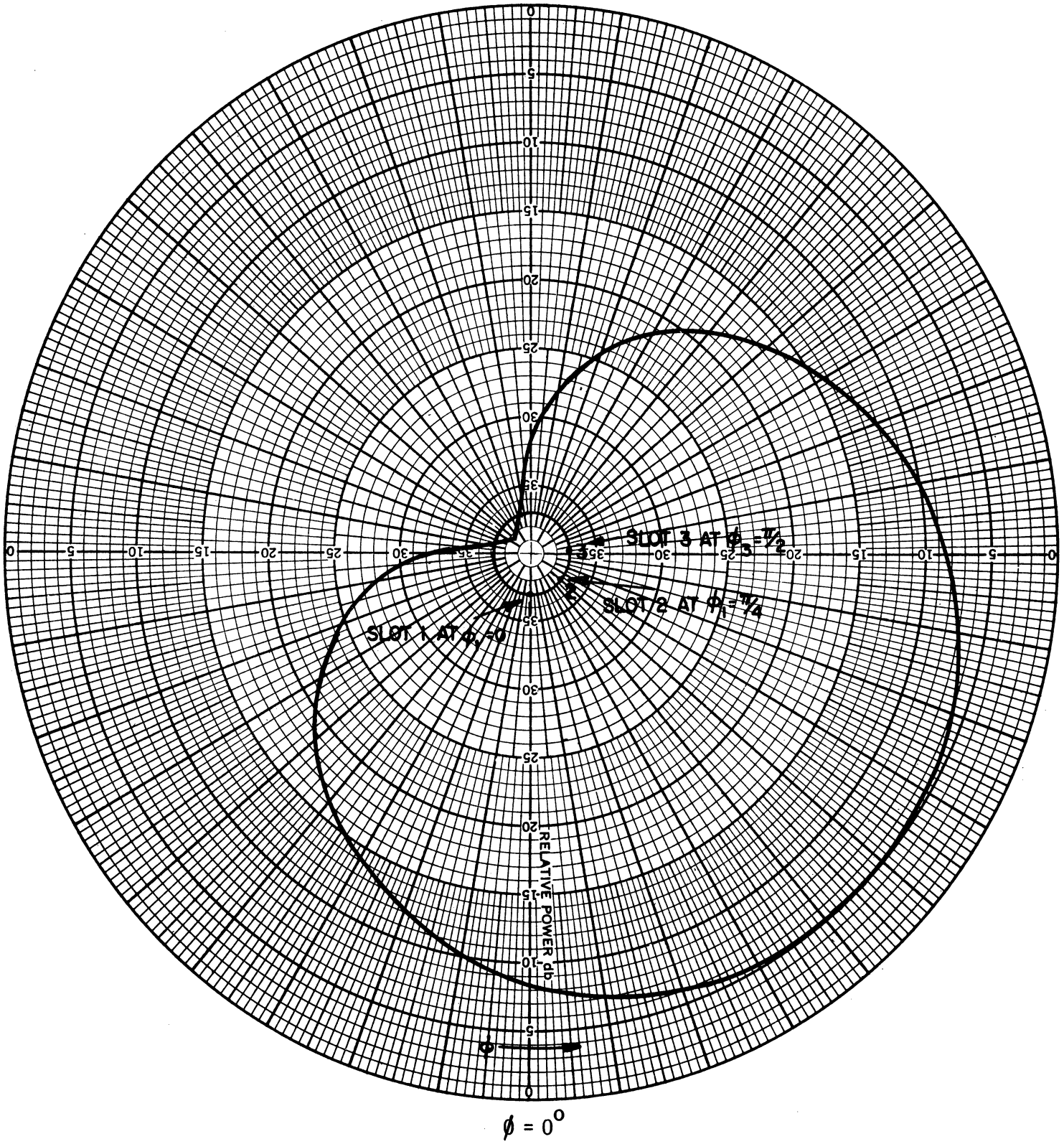

Figure 7(b): Theoretical patterns of three axial slots located on the surface of a conducting cylinder, $ka = \pi/\sqrt{2}$, $V_1 = V_3 = 0.5$, $V_1 = 1.0$, $\psi_2 = ka$, $\psi_1 = \psi_3 = ka/\sqrt{2}$.

Figures 8 (a)-(c) show the patterns produced by the 4-slot array located on a cylinder for various values of ka. Observe that for $ka = 0.8\pi$ (Figure 8(b)) the field in $\phi = -45^{o}$ region is about 30dB down from that at the maximum. For $ka = 1.0\pi$ (Figure 8(c)) the field in the $\phi \simeq 45^{o}$ region is about 17dB down while for $ka = 0.4\pi$ the pattern is not much different from that of a single slot on a cylinder discussed earlier.

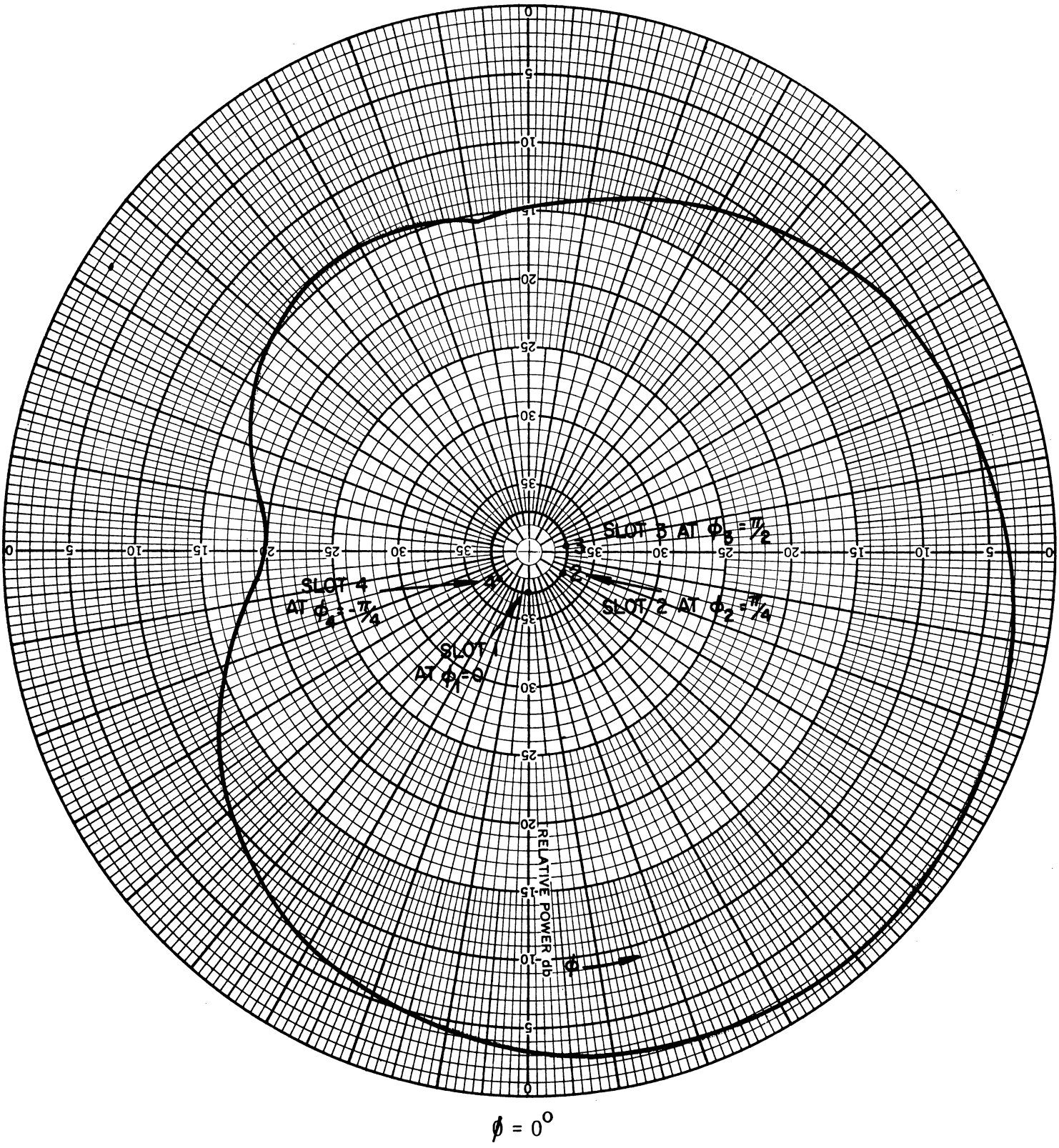

Figure 8(a): Theoretical pattern of four axial slots located on the surface of a conducting cylinder, $ka = 0.4\pi$, $V_1 = V_2 = V_3 = 1.0$, $V_4 = 0.25$, $\psi_1 = \psi_3 = ka/\sqrt{2}$, $\psi_2 = ka$, $\psi_4 = 0$.

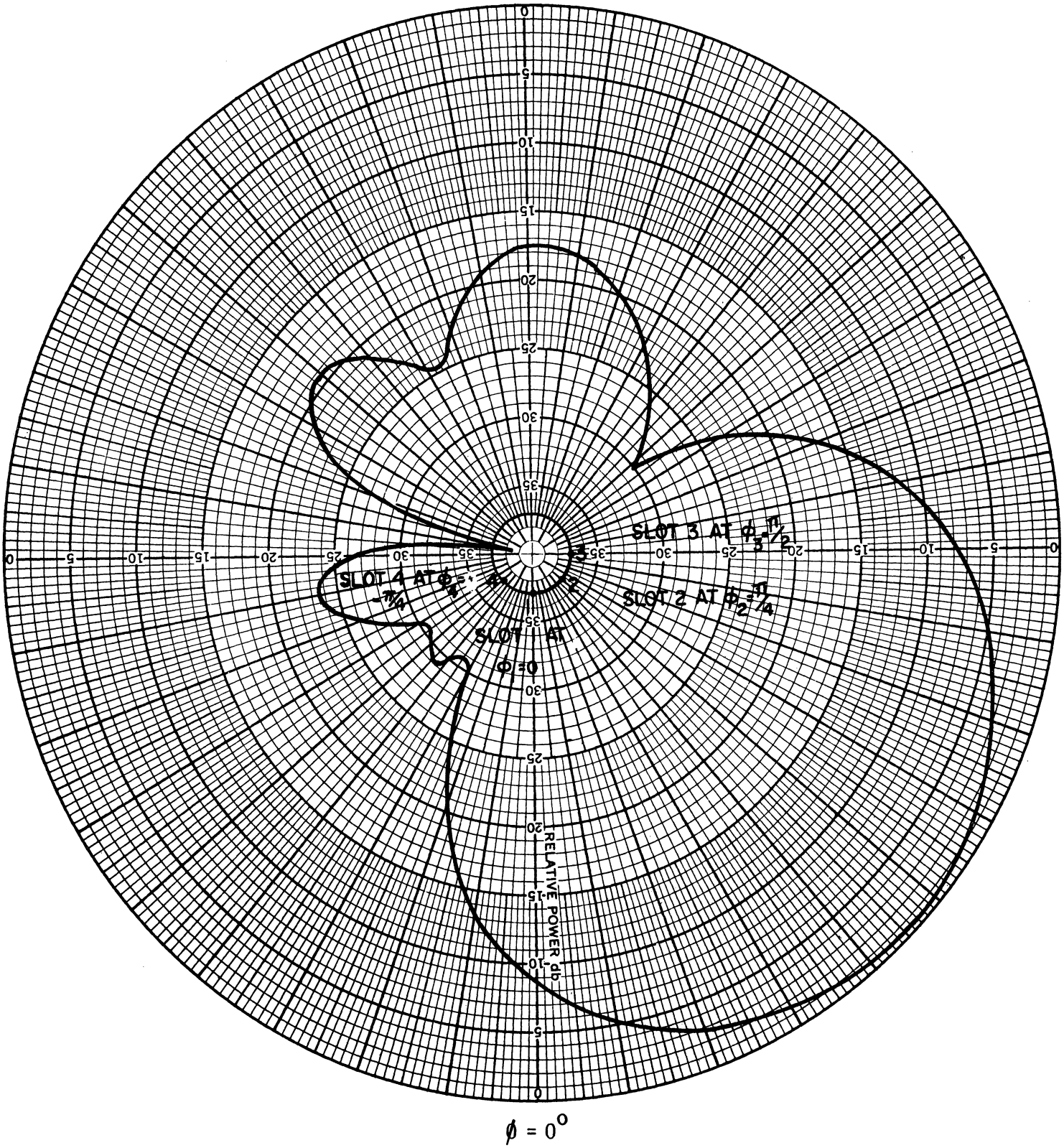

Figure 8(b): Theoretical pattern of four axial slots located on the surface of a conducting cylinder, ka = 0.8π, $V_1 = V_2 = V_3 = 1.0$, $V_4 = 0.25$, $\psi_1 = \psi_3 = ka/\sqrt{2}$, $\psi_2 = ka$, $\psi_4 = 0$.

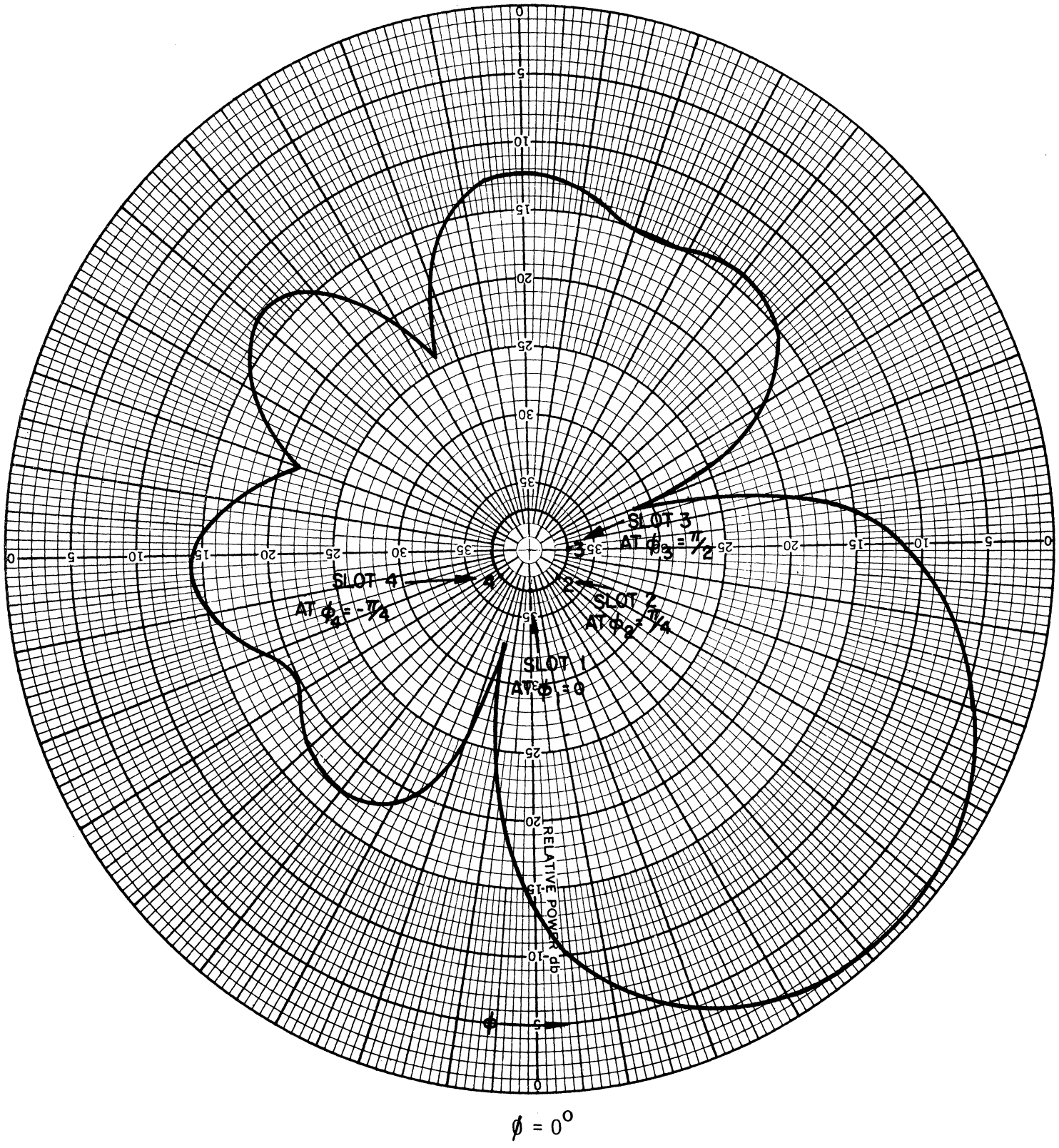

Figure 8(c): Theoretical pattern of four axial slots located on the surface of a conducting cylinder, $ka = 1.0\pi$, $V_1 = V_2 = V_3 = 1.0$, $V_4 = 0.25$, $\psi_1 = \psi_3 = ka/\sqrt{2}$, $\psi_2 = ka$, $\psi_4 = 0$.

III EXPERIMENTAL RESULTS AND COMPARISON WITH THEORY

3.1 Elementary Slot

As mentioned earlier, the elementary radiator used is a magnetic dipole or a slot. The experimental model may be fabricated out of stripline. The slot has the advantage that it requires minimum protrusions when mounted on the cylinder surface. Figures 9a and 9b show the photographs of the front and back sides of the stripline slot radiator. The measured x-y plane pattern of the slot on a cylinder with ka $\simeq 1.387\pi$ is shown in Figure 10. The corresponding theoretical pattern is also shown in Figure 10. The agreement between theory and experiment may be considered to be satisfactory. It has been found that for a slot of length approximately equal to a wavelength, the input VSWR stays within 1:3 in the frequency range of 2.8 - 3.4 GHz.

3.2 3-Slot Array

A photograph of the 3-slot array mounted on the cylinder is shown in Figure 11(a). An array of 3 axial slots mounted on a cylinder with ka -1.4π has been fabricated. For mechanical simplicity the individual slots in Figure 11(a) are made of reduced height waveguide sections. Figure 11(b) shows a sketch of a slot on the broad wall of a cavity made of reduced height waveguide. The system is fed by a coaxial probe as shown. The impedance characteristics of the slot depends critically on the locations of the slot and the height of the waveguide. The measured x-y plane pattern of the antenna is shown in Figure 12. The results shown in Figure 12 agree fairly well with the theoretical pattern discussed in section 2.6. During the experiment the three slots were fed by a 3-way power divider and phasing of the slots were done with the help of appropriate length of transmissinn line. The measured input VSWR as a function of frequency for the 3-slot antenna is shown in Table I.

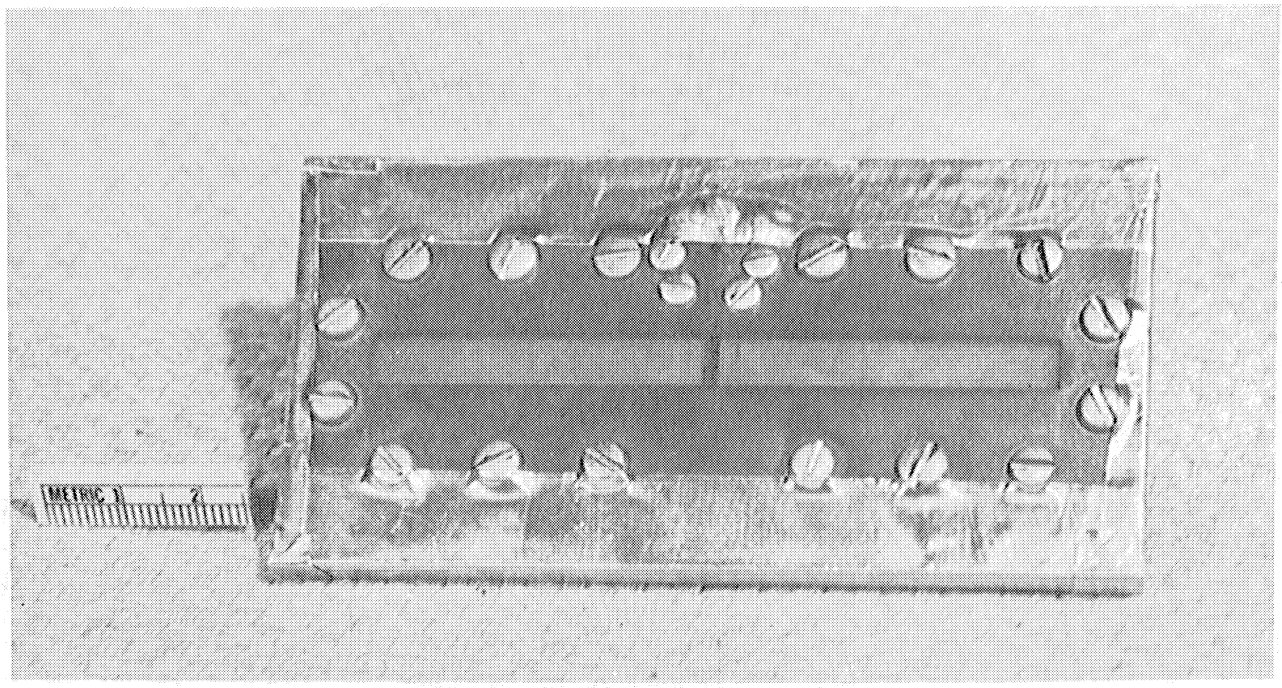

Figure 9(a): Photograph of the front side of the stripline slot radiator.

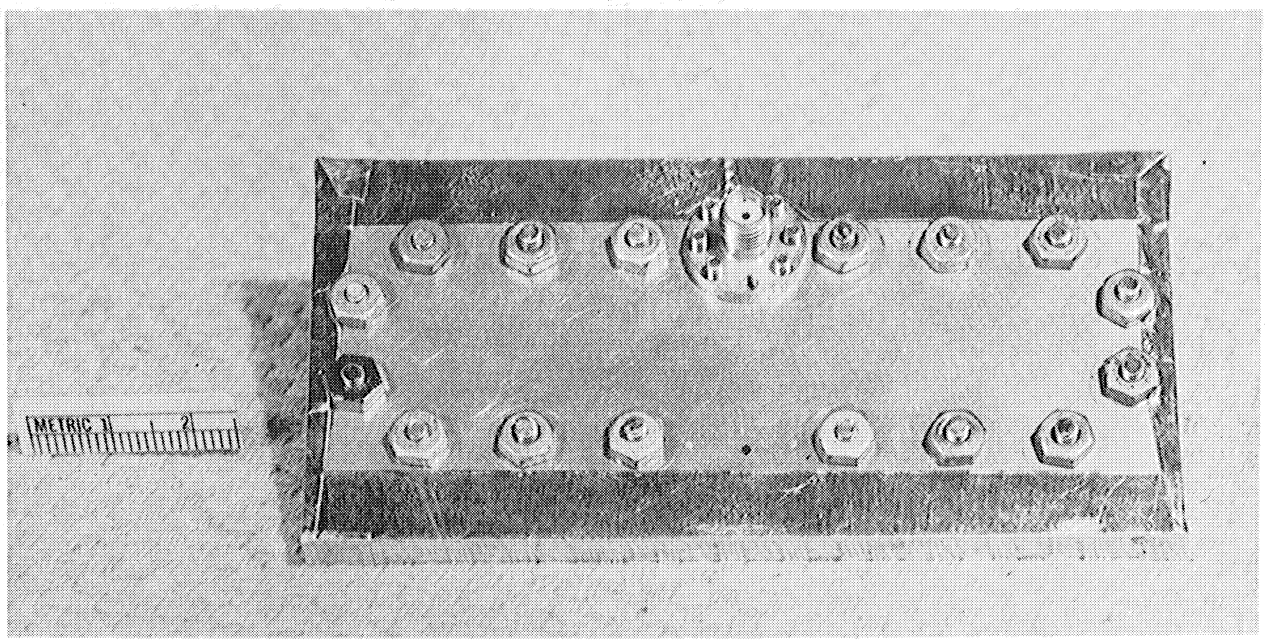

Figure 9(b): Photograph of the back side of the stripline slot radiator.

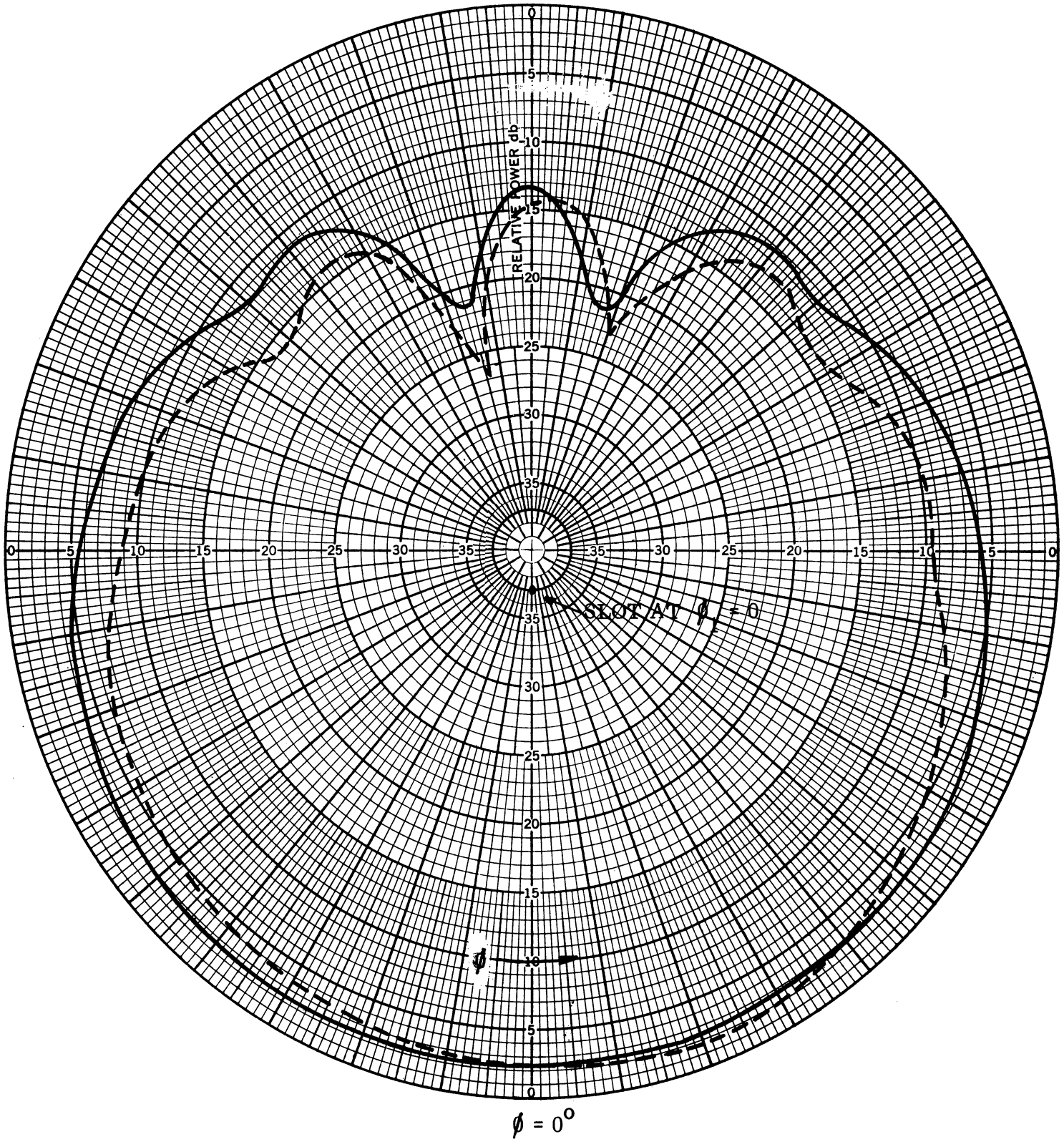

Figure 10: Patterns of an axial slot on the surface of a conducting cylinder, ka = 1.397π. —— theoretical ----- experimental.

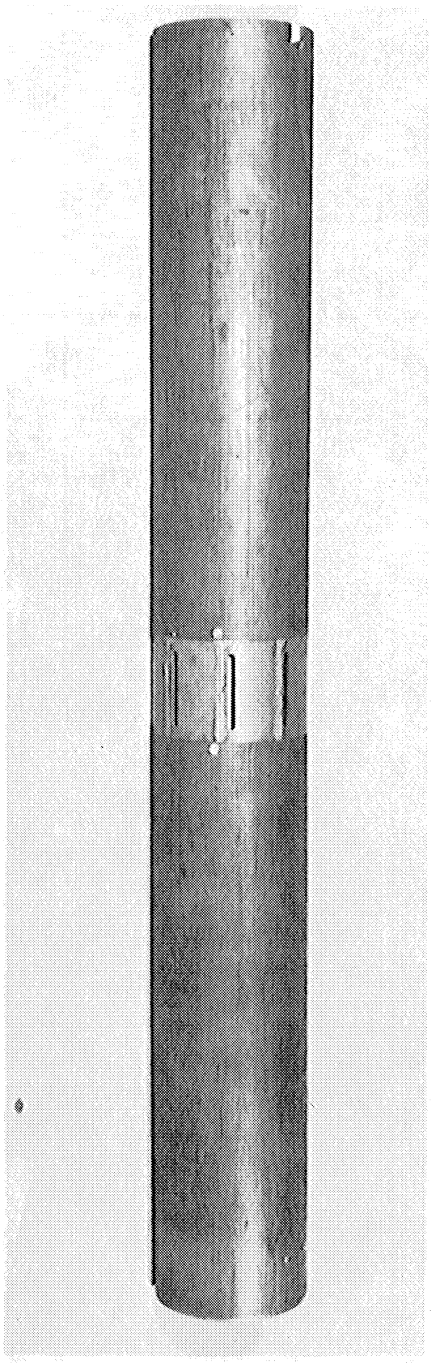

Figure 11(a): A photograph of the 3-slot array mounted on a conducting cylinder.

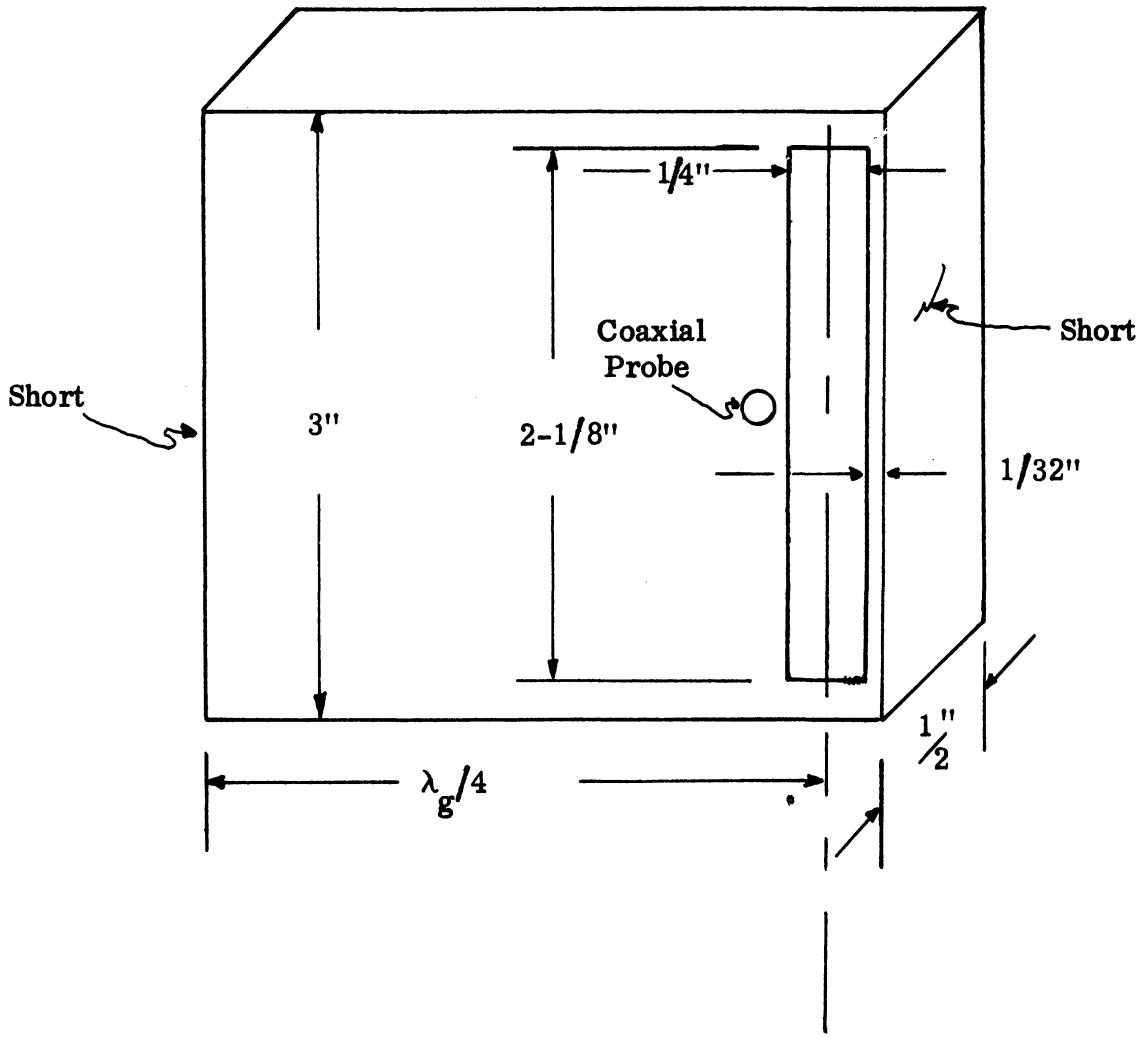

Figure 11(b): Sketch of a slot on the broad face of a reduced height waveguide cavity.

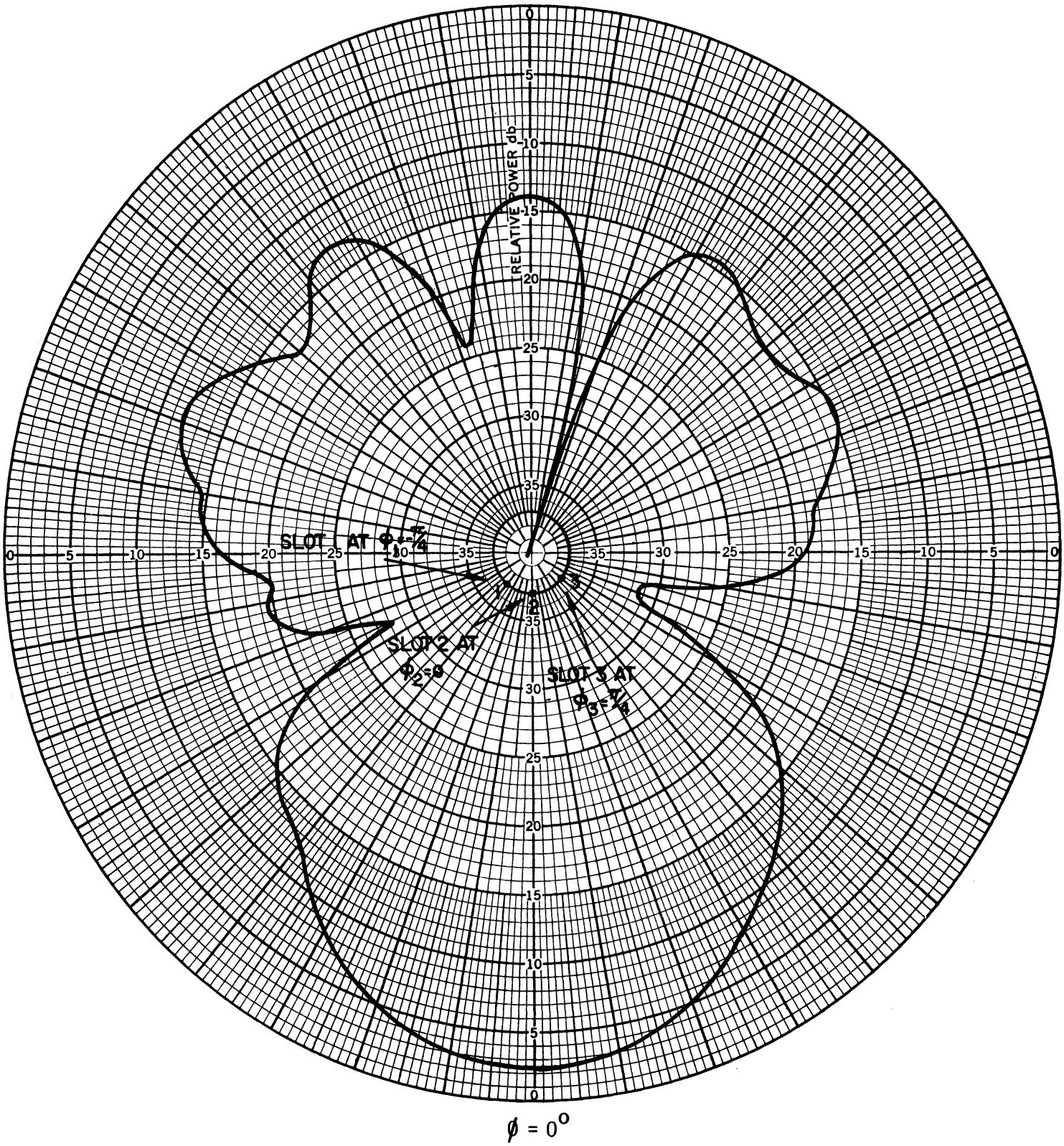

Figure 12: Experimental pattern of three axial slots located on the surface of a conducting cylinder, ka $\simeq 1.4\pi$, $V_1 = V_2 = V_3 = 1.0$, $\psi_1 = \psi_3 \simeq ka/\sqrt{2}$, $\psi_2 \simeq ka$, f = 3.5 GHz.

Table I. Input VSWR for the 3-slot array.

Frequency (GHz)	VSWR
2.9	1.06
3.0	1.06
3.1	1.06
3.2	1.08
3.3	1.14
3.4	1.18
3.5	1.31
3.6	1.36
3.7	1.43

It may be of some interest to know the VSWR at the input of each slot and this data are shown in Table II below.

Table II. VSWR at the input of each slot.

Frequency (GHz)	Slot 1	Slot 2	Slot 3
3.0	3.9	3.8	3.6
3.2	1.95	2.4	1.95
3.3	1.39	1.56	1.34
3.4	1.65	1.60	1.57
3.5	2.4	2.39	2.4

The results given in Tables I and II indicate that the input end of the power divider is well matched. This was achieved by designing the power divider such that the impedance of each slot is properly matched to the power divider.

3.3 The 4-Slot Array

The individual slots of the 4-slot array are made of reduced height waveguide as in Figure 11(a). Figures 13(a)-(e) show the experimental and theoretical x-y plane patterns of the antenna at different frequencies. The

slots were fed by 4-way power dividers to provide the appropriate amplitude of excitation. The phasing was done by appropriate amount of line length. The agreement between theoretical and experimental patterns shown in Figure 13 may be considered to be satisfactory. The measured cross-polarization patterns of the antenna over the same frequency range are shown in Figure 14 (a)-(e). Typically at f = 3.1 GHz the cross-polarization component is about 25dB down in the direction of the beam maximum. In other directions the cross-polarization response is lower than 25dB. The input VSWR as a function of frequency is shown in Table III.

Table III. Input VSWR for the 4-slot array.

Frequency (GHz)	VSWR
3.1	1.38
3.2	1.05
3.3	1.26
3.4	1.60
3.5	1.68

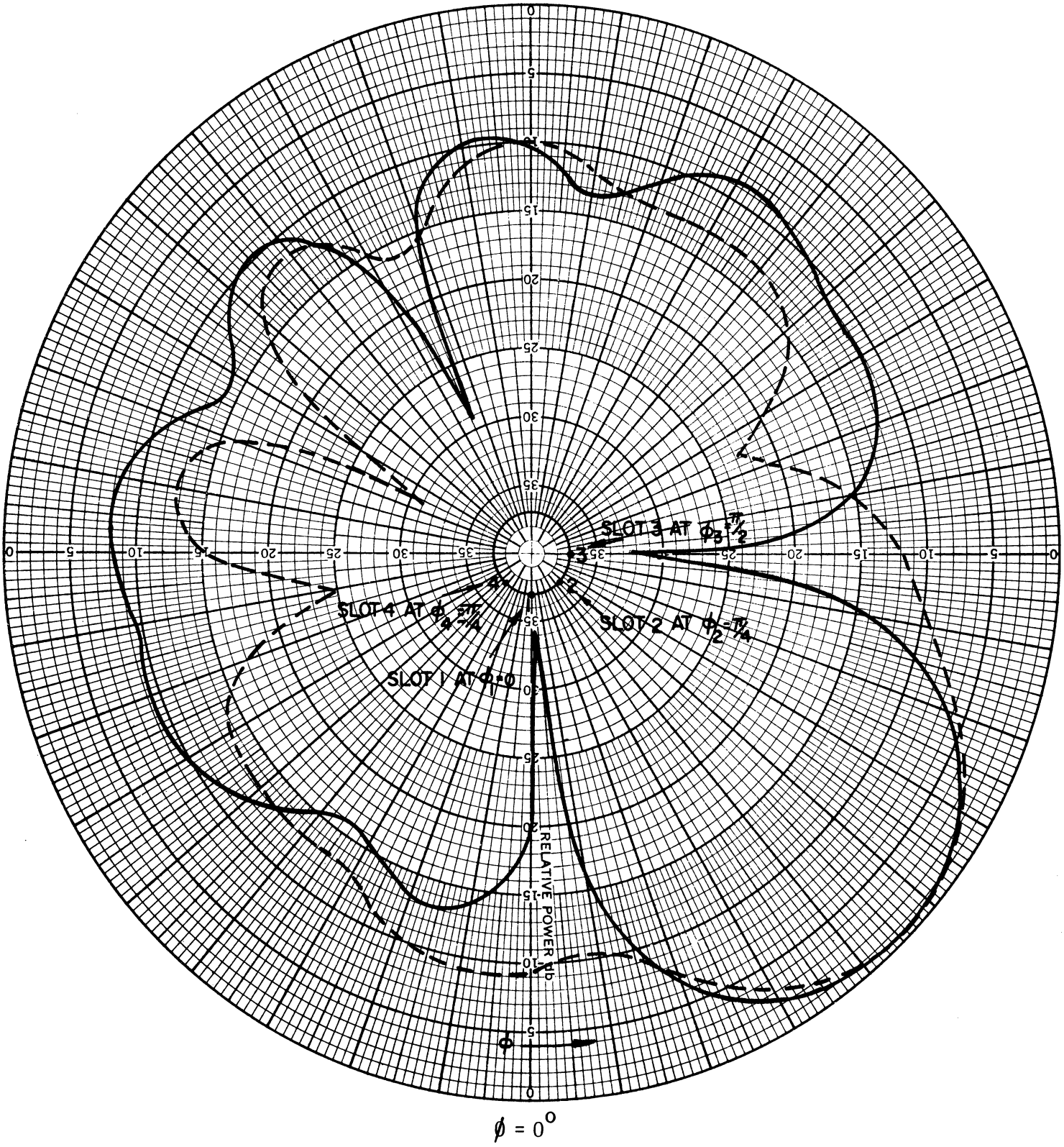

Figure 13(a): Patterns of an array of 4 axial slots on the surface of a conducting cylinder, ka = 1.312π, f = 3.1 GHz, $V_1 = V_2 = V_3 = 1.0$, $V_4 = 0.4$, $\psi_1 = \psi_3 = ka/\sqrt{2}$, $\psi_2 = ka$, $\psi_4 = 0$. ——— theoretical ----- experimental.

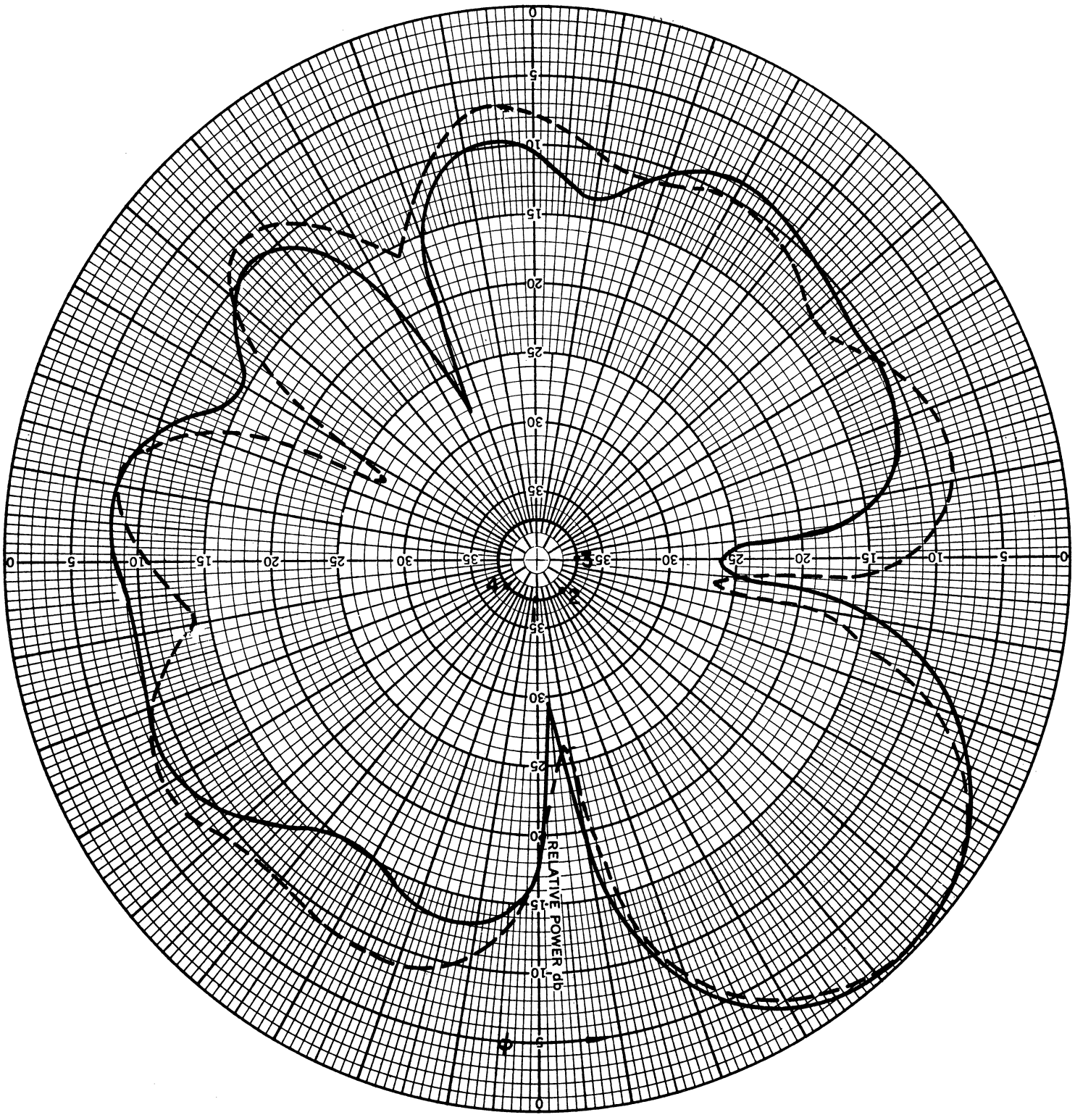

Figure 13(b): Patterns of an array of 4 axial slots on the surface of a conducting cylinder, $ka = 1.354\pi$, $f = 3.2$ GHz, $V_1 = V_2 = V_3 = 1.0$, $V_4 = 0.4$, $\psi_1 = \psi_3 = ka/\sqrt{2}$, $\psi_2 = ka$, $\psi_4 = 0$. —— theoretical ------ experimental.

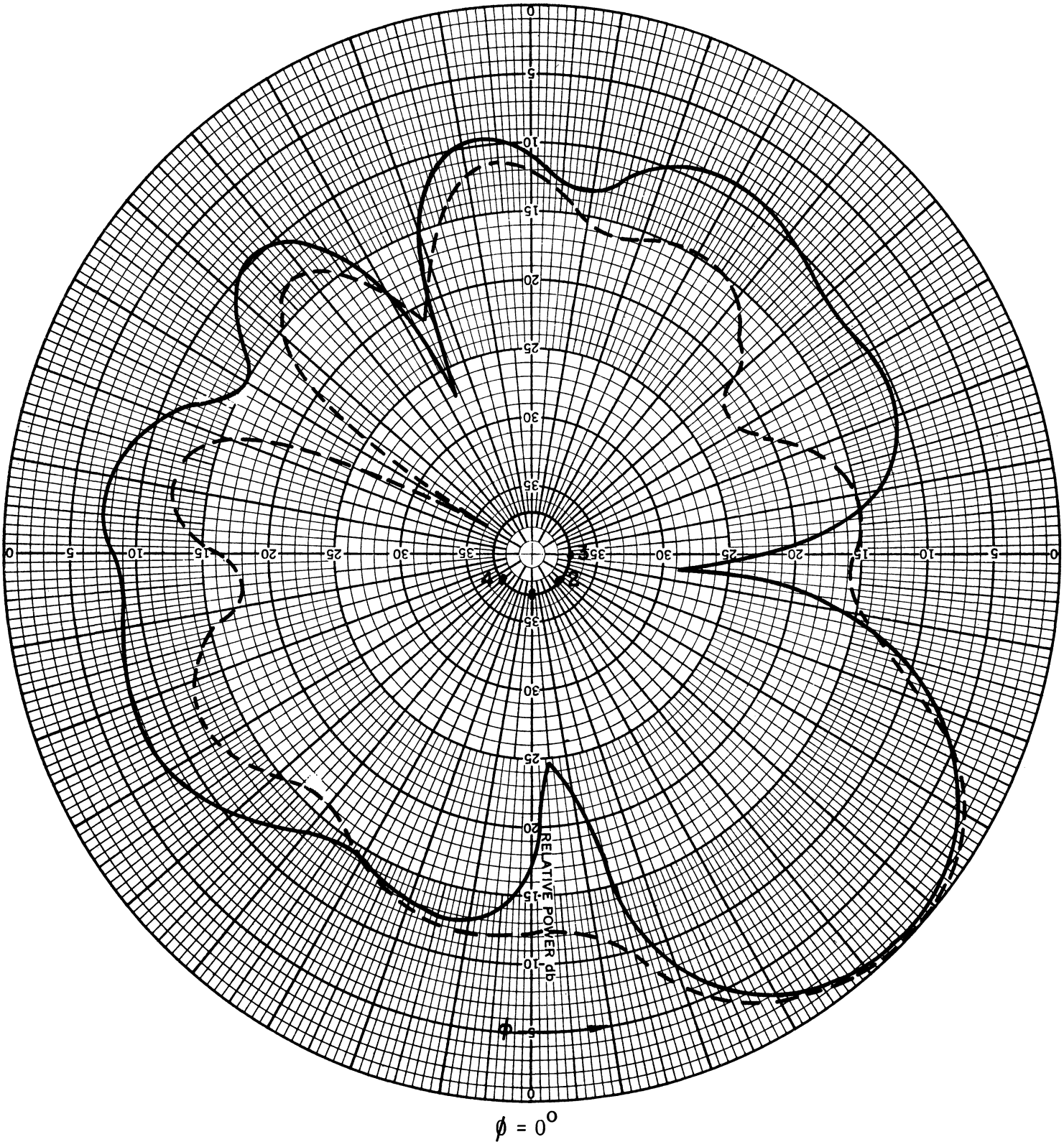

Figure 13(c): Patterns of an array of 4 axial slots on the surface of a conducting cylinder, ka = 1.396π, f = 3.3 GHz, $V_1 = V_2 = V_3 = 1.0$, $V_4 = 0.4$, $\psi_1 = \psi_3 = ka/\sqrt{2}$, $\psi_2 = ka$, $\psi_4 = 0$. —— theoretical ----- experimental.

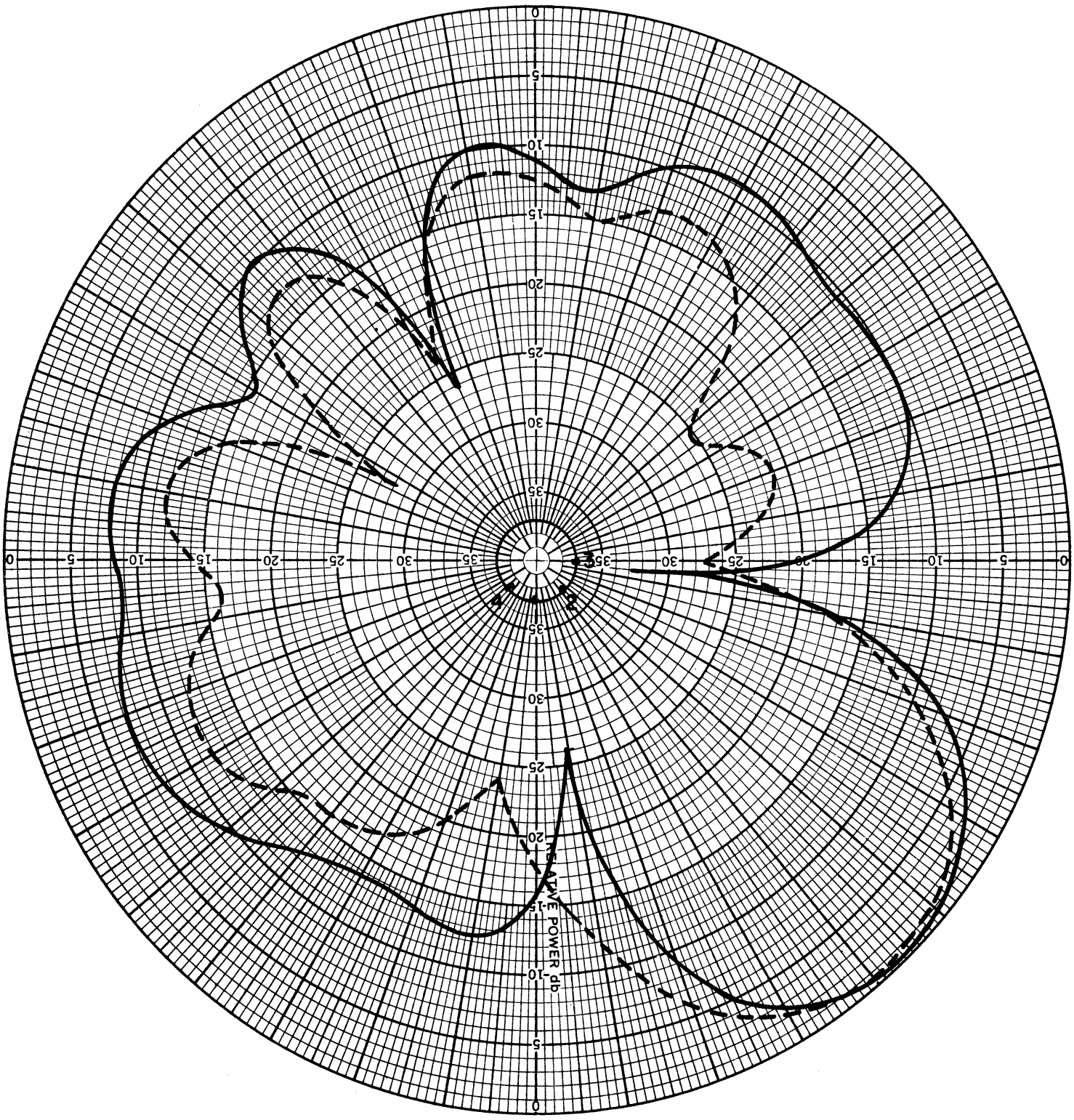

Figure 13(d): Patterns of an array of 4 axial slots on the surface of a conducting cylinder, ka = 1.439π, f = 3.4 GHz, $V_1 = V_2 = V_3 = 1.0$, $V_4 = 0.4$, $\psi_1 = \psi_3 = ka/2$, $\psi_2 = ka$, $\psi_4 = 0$. —— theoretical ----- experimental.

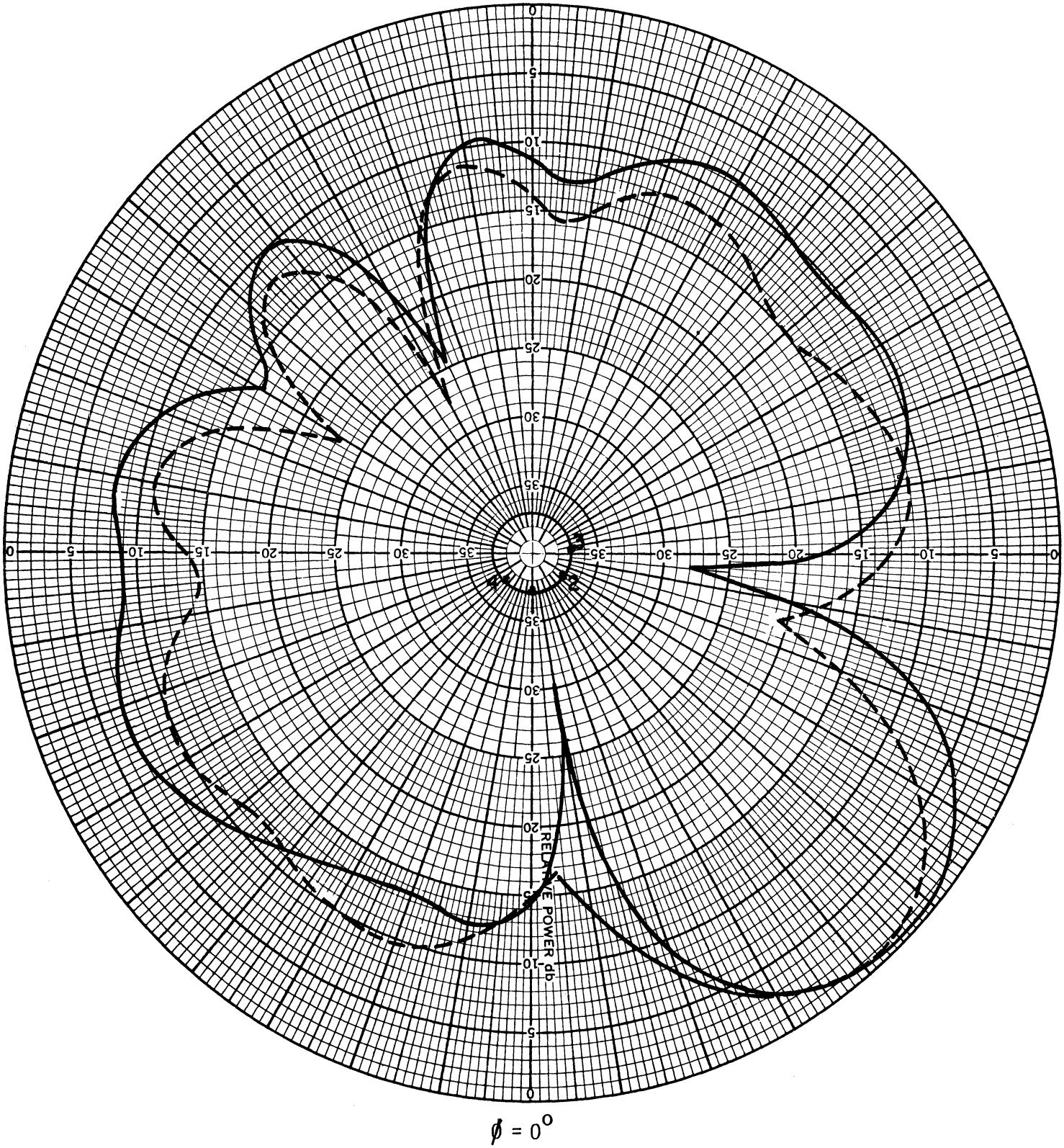

Figure 13(e): Patterns of an array of 4 axial slots on the surface of a conducting cylinder, $ka = 1.481\pi$, $f = 3.5$ GHz, $V_1 = V_2 = V_3 = 1.0$, $V_4 = 0.4$, $\psi_1 = \psi_3 = ka/\sqrt{2}$, $\psi_2 = ka$, $\psi_4 = 0$. —— theoretical ----- experimental.

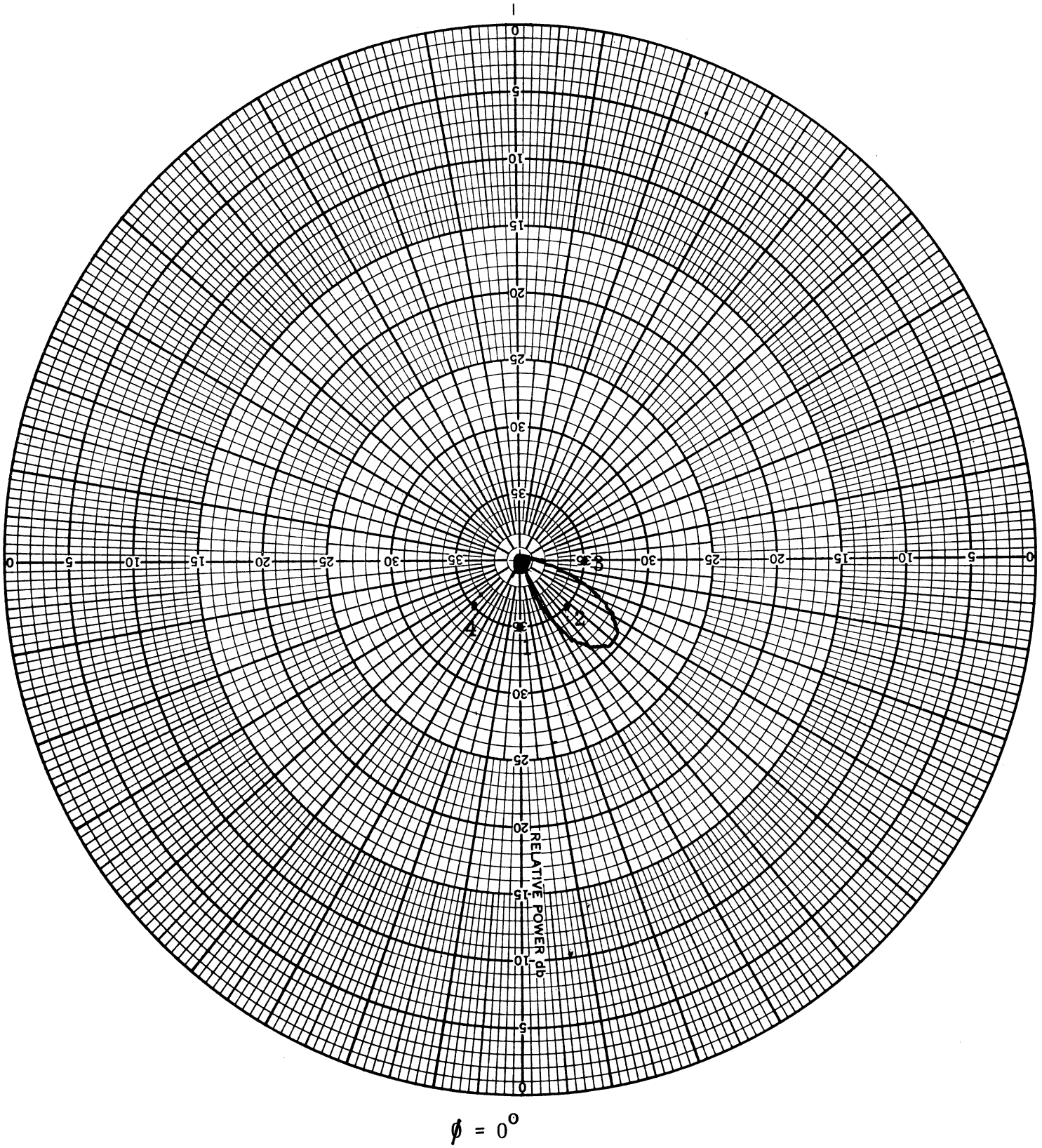

$\phi = 0^{o}$

Figure 14(a): Measured cross-polarization pattern of an array of 4 axial slots on the surface of a conducting cylinder. ka = 1.312π, f = 3.1 GHz, $V_1 = V_2 = V_3 = 1.0$, $V_4 = 0.4$, $\psi_1 = \psi_3 = ka/\sqrt{2}$, $\psi_2 = ka$, $\psi_4 = 0$. Maximum cross-polarization $\simeq$ -25dB down.

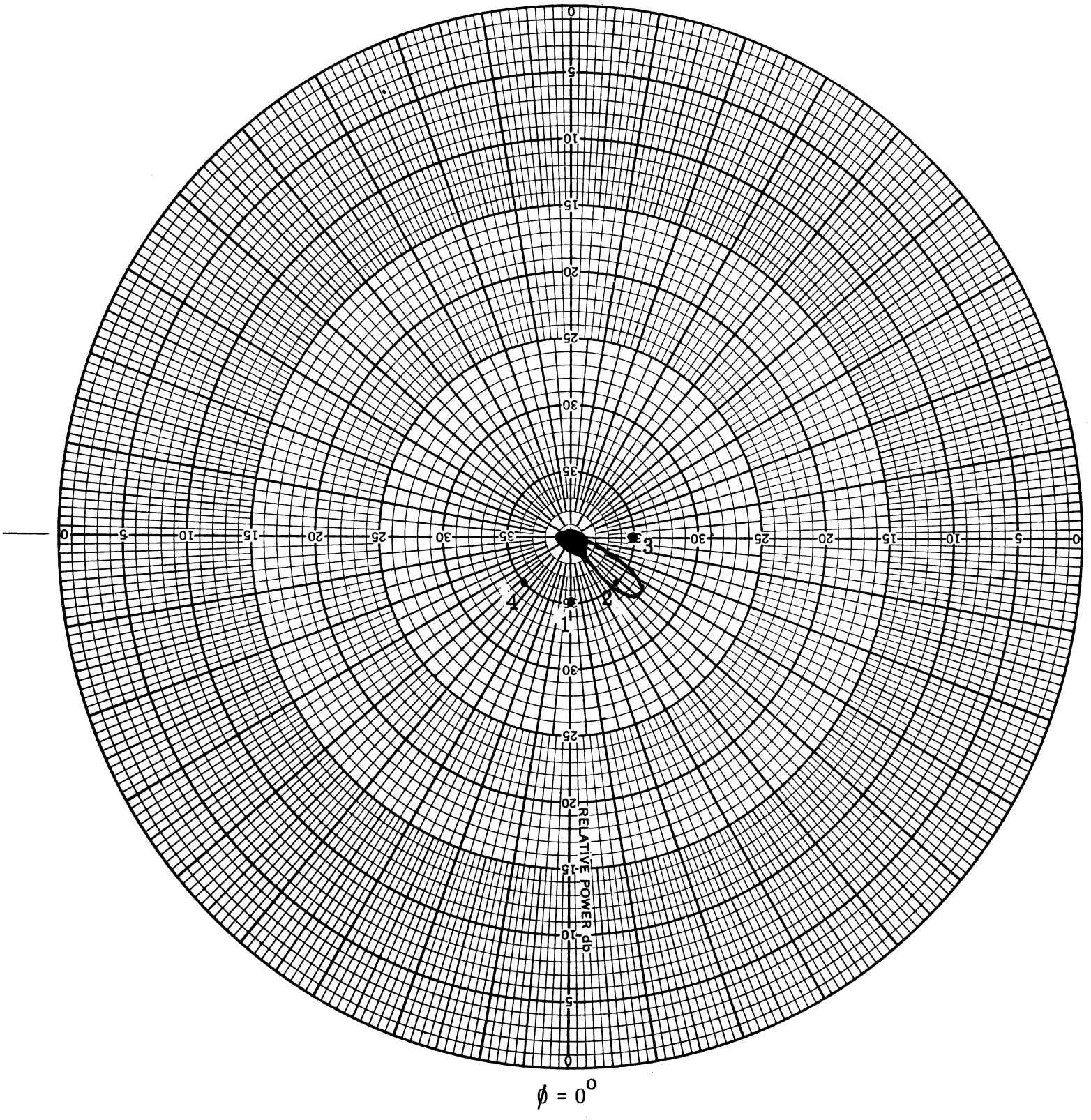

Figure 14(b): Measured cross-polarization pattern of an array of 4 axial slots on the surface of a conducting cylinder. ka = 1.354π, f = 3.2 GHz, $V_1 = V_2 = V_3 = 1.0$, $V_4 = 0.4$, $\psi_1 = \psi_3 = ka/\sqrt{2}$, $\psi_2 = ka$, $\psi_4 = 0$. Maximum cross-polarization $\simeq$ -26.5dB down.

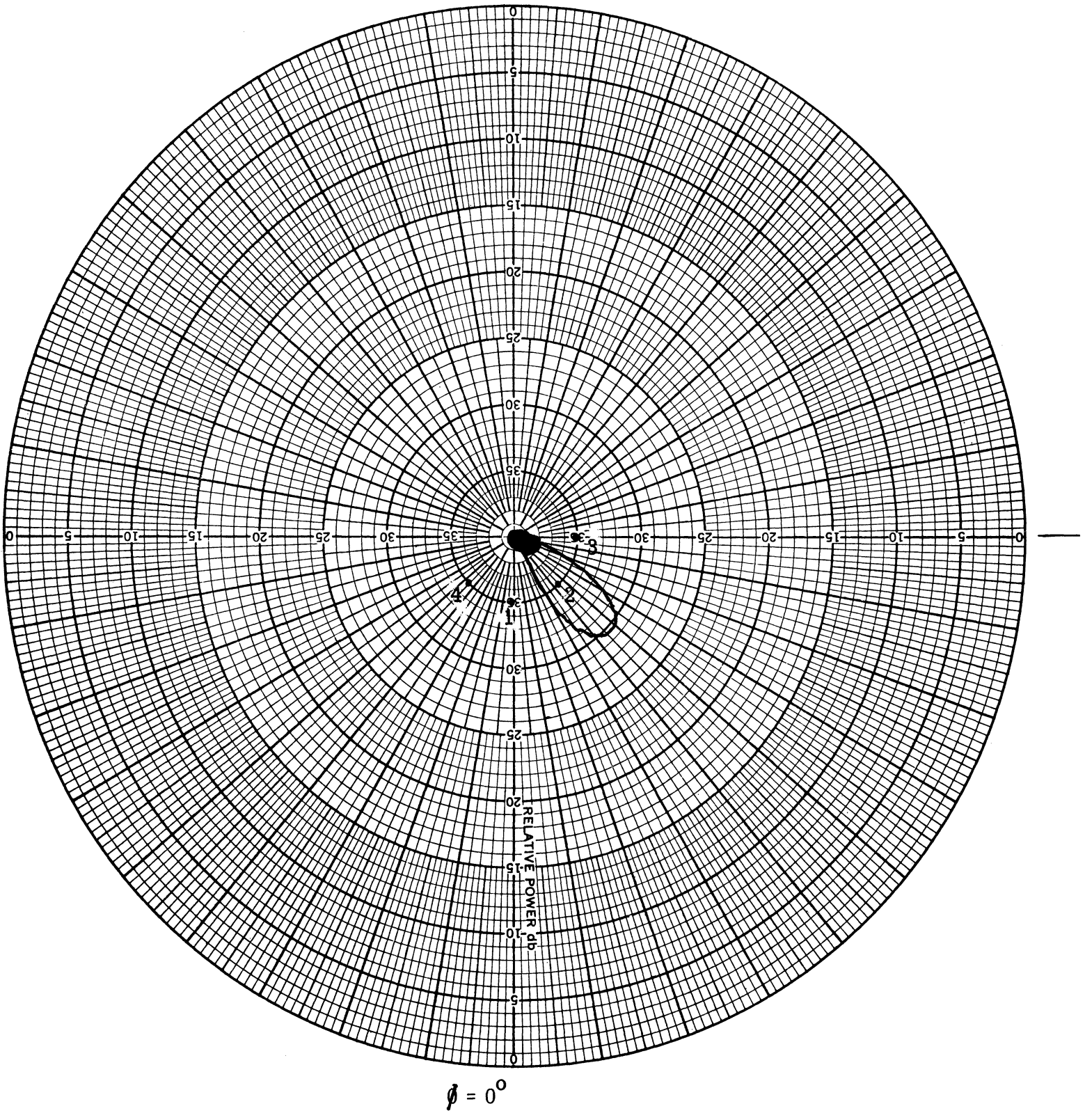

Figure 14(c): Measured cross-polarization pattern of an array of 4 axial slots on the surface of a conducting cylinder. $ka = 1.396\pi$, $f = 3.3$ GHz, $V_1 = V_2 = V_3 = 1.0$, $V_4 = 0.4$, $\psi_1 = \psi_3 = ka/\sqrt{2}$, $\psi_2 = ka$, $\psi_4 = 0$. Maximum cross-polarization $\simeq$ -27.5dB.

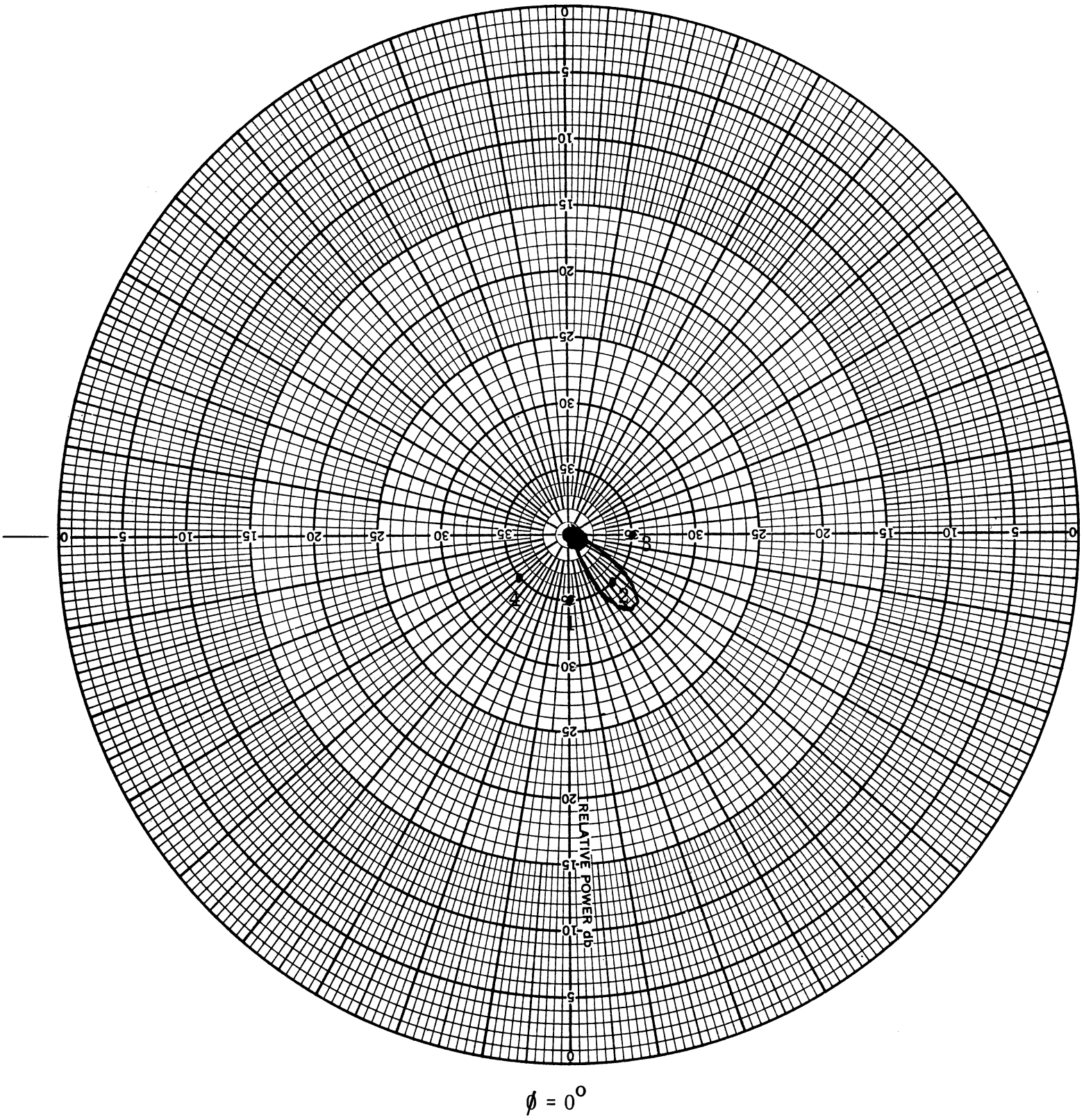

$\phi = 0^{o}$

Figure 14(d): Measured cross-polarization pattern of an array of 4 axial slots on the surface of a conducting cylinder. ka = 1.439π, f = 3.4 GHz, $V_1 = V_2 = V_3 = 1.0$, $V_4 = 0.4$, $\psi_1 = \psi_3 = ka/\sqrt{2}$, $\psi_2 = ka$, $\psi_4 = 0$. Maximum cross-polarization $\simeq$ -26.0dB.

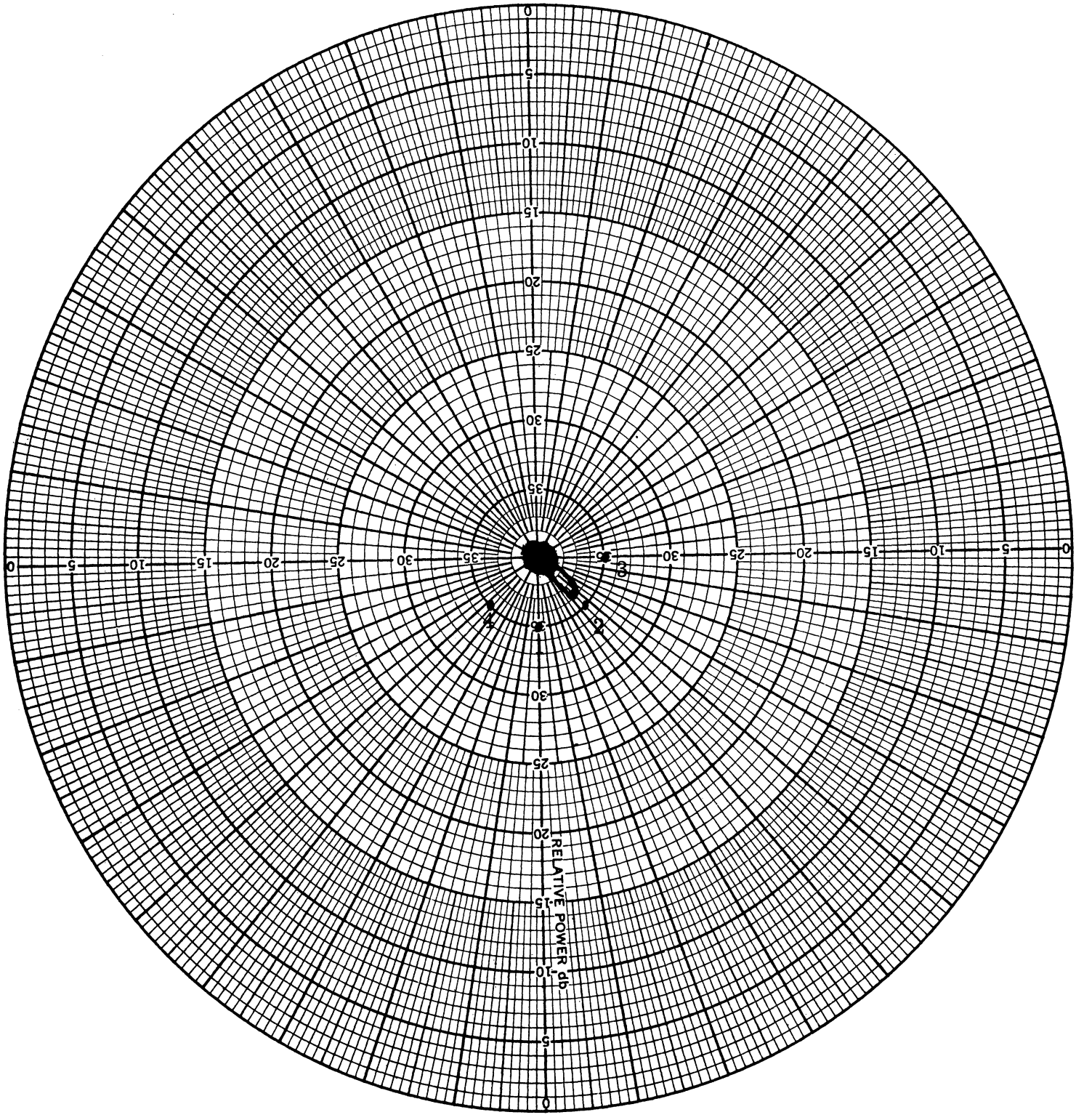

$\phi = 0^{o}$

Figure 14(e): Measured cross-polarization pattern of an array of 4 axial slots on the surface of a conducting cylinder. $ka = 1.481\pi$, $f = 3.5$ GHz, $V_1 = V_2 = V_3 = 1.0$, $V_4 = 0.4$, $\psi_1 = \psi_3 = ka/\sqrt{2}$, $\psi_4^1 = 0^2$. Maximum cross-polarization $\simeq$ -30.0dB.

IV CONCLUSIONS

The results of the theoretical and experimental investigation discussed in the previous sections indicate that it is possible to obtain a single beam pattern with the help of an array of axial slots on a circular cylinder. However, it appears from the results that the pattern will not be optimum at the lower end of the frequency band for the given size of the cylinder. The VSWR results indicate that it would be possible to achieve the design goal of 1:3 VSWR over the band of frequencies of interest.

In an extension of this work it is recommended that the following studies should be performed:

(i) Re-design the array so as to illuminate a region, perhaps 30^{o} to 75^{o}, as measured from the nadir.

(ii) Establish a lower frequency limit in terms of cylinder diameter/λ, for which it is possible to obtain a 10dB difference in the illumination over the 30^{o} to 75^{o} angle spread. The discrimination is to be between the illuminated side and the corresponding same angle on the shadowed side.

(iii) Slot spacings other than $\pi/4$ investigated.

(iv) Determine the effects of the waveguide height on the impedance characteristics of the individual slot.

(v) Experimental studies to verify some of the findings of the theory for the re-designed array.

REFERENCES

[1] J.R. Wait (1959), Electromagnetic Radiation from Cylindrical Structures, Pergamon Press, N.Y.

[2] R.F. Collin and F.J. Zucker (1969), Antenna Theory, Part I, McGraw-Hill Book Co., New York.

[3] J.J. Bowman, T.B.A. Senior and P.L.E. Uslenghi (1969), Electro-Magnetic and Acoustic Scattering by Simple Shapes, North Holland Publishing Co., Amsterdam.

[4] D.L. Sengupta (1974), "VHF Antenna for Electrically Small Vehicles", Quarterly Status Report No. 1, Contract F19628-74-C-0020, The University of Michigan Radiation Laboratory, Ann Arbor, MI. 48105.